AMERICAN SOCIETY FOR MICROBIOLOGY | mBio®

Fusobacterium nucleatum Secretes Outer Membrane Vesicles and Promotes Intestinal Inflammation

Melinda A. Engevik,[a,b] Heather A. Danhof,[c] Wenly Ruan,[d] Amy C. Engevik,[e] Alexandra L. Chang-Graham,[c] Kristen A. Engevik,[c] Zhongcheng Shi,[a,b] Yanling Zhao,[f] Colleen K. Brand,[c] Evan S. Krystofiak,[g] Susan Venable,[a,b] Xinli Liu,[h] Kendal D. Hirschi,[i] Joseph M. Hyser,[c] Jennifer K. Spinler,[a,b] Robert A. Britton,[c] James Versalovic[a,b]

aDepartment of Pathology and Immunology, Baylor College of Medicine, Houston, Texas, USA
bDepartment of Pathology, Texas Children's Hospital, Houston, Texas, USA
cDepartment of Molecular Virology and Microbiology, Baylor College of Medicine, Houston, Texas, USA
dDepartment of Pediatrics, Baylor College of Medicine, Houston, Texas, USA
eDepartment of Surgical Sciences, Vanderbilt University Medical Center, Nashville Tennessee, USA
fDepartment of Pediatrics, Texas Children's Cancer Center, Texas Children's Hospital, Houston, Texas, USA
gDepartment of Cell and Developmental Biology, Vanderbilt University, Nashville, Tennessee, USA
hDepartment of Pharmacological and Pharmaceutical Sciences, University of Houston, Houston, Texas, USA
iDepartment of Pediatrics and Human and Molecular Genetics, Children's Nutrition Research Center, Baylor College of Medicine, Houston, Texas, USA

ABSTRACT Multiple studies have implicated microbes in the development of inflammation, but the mechanisms remain unknown. Bacteria in the genus *Fusobacterium* have been identified in the intestinal mucosa of patients with digestive diseases; thus, we hypothesized that *Fusobacterium nucleatum* promotes intestinal inflammation. The addition of >50 kDa *F. nucleatum* conditioned media, which contain outer membrane vesicles (OMVs), to colonic epithelial cells stimulated secretion of the proinflammatory cytokines interleukin-8 (IL-8) and tumor necrosis factor (TNF). In addition, purified *F. nucleatum* OMVs, but not compounds <50 kDa, stimulated IL-8 and TNF production; which was decreased by pharmacological inhibition of Toll-like receptor 4 (TLR4). These effects were linked to downstream effectors p-ERK, p-CREB, and NF-κB. *F. nucleatum* >50-kDa compounds also stimulated TNF secretion, p-ERK, p-CREB, and NF-κB activation in human colonoid monolayers. In mice harboring a human microbiota, pretreatment with antibiotics and a single oral gavage of *F. nucleatum* resulted in inflammation. Compared to mice receiving vehicle control, mice treated with *F. nucleatum* showed disruption of the colonic architecture, with increased immune cell infiltration and depleted mucus layers. Analysis of mucosal gene expression revealed increased levels of proinflammatory cytokines (KC, TNF, IL-6, IFN-γ, and MCP-1) at day 3 and day 5 in *F. nucleatum*-treated mice compared to controls. These proinflammatory effects were absent in mice who received *F. nucleatum* without pretreatment with antibiotics, suggesting that an intact microbiome is protective against *F. nucleatum*-mediated immune responses. These data provide evidence that *F. nucleatum* promotes proinflammatory signaling cascades in the context of a depleted intestinal microbiome.

IMPORTANCE Several studies have identified an increased abundance of *Fusobacterium* in the intestinal tracts of patients with colon cancer, liver cirrhosis, primary sclerosing cholangitis, gastroesophageal reflux disease, HIV infection, and alcoholism. However, the direct mechanism(s) of action of *Fusobacterium* on pathophysiological within the gastrointestinal tract is unclear. These studies have identified that *F. nucleatum* subsp. *polymorphum* releases outer membrane vesicles which activate TLR4 and NF-κB to stimulate proinflammatory signals *in vitro*. Using mice harboring a human microbiome, we demonstrate that *F. nucleatum* can promote inflammation, an effect which required antibiotic-mediated alterations in the gut microbiome. Collectively, these results suggest a mechanism by which *F. nucleatum* may contribute to intestinal inflammation.

Recently, it has been hypothesized that the oral cavity may serve as a reservoir for potential pathobionts that can exacerbate intestinal disease (1–4). In support of this hypothesis, increased abundances of oral microbes, including *Fusobacterium* spp, have been reported in the intestines of patients with colon cancer, primary sclerosing cholangitis, gastroesophageal reflux disease, HIV infection, alcoholism, and inflammatory bowel disease (IBD) (2, 5–21). In patients with IBD, an increased abundance of *Fusobacterium* spp. has been identified in biopsy specimens (6, 10–20), and the presence of *Fusobacterium* strongly correlates with disease status (6). *Fusobacterium* is an anaerobic, Gram-negative opportunistic pathogen from the *Fusobacteriaceae* family that can cause several human diseases, including periodontal disease, intrauterine infection, Lemierre's syndrome, skin ulcers, and appendicitis (22–28). Of the *Fusobacterium* species, *F. nucleatum* has recently emerged as a compelling candidate for causing human diseases given its prevalence in tissue specimens (10, 11, 14). In colorectal cancer, *F. nucleatum* promotes a NF-κB-driven proinflammatory genetic signature, including tumor necrosis factor (TNF) and interleukin-6 (IL-6) gene expression (29, 30), cytokines that are also important in intestinal inflammation. Despite the relative abundance of *Fusobacterium* species in gastrointestinal diseases, the literature to date has focused on intestinal *F. nucleatum* in colorectal cancer. Whether *F. nucleatum* is also a driver of intestinal inflammation in the normal gut represents a major gap in knowledge.

Liu et al. demonstrated that *F. nucleatum* produces outer membrane vesicles (OMVs) (31), nanoparticles that are naturally secreted by Gram-negative bacteria. OMVs typically contain antigenic components that can activate Toll-like receptors (TLRs) on epithelial cells or immune cells. TLR activation is linked to activation of the NF-κB pathway and elicitation of proinflammatory cytokine release. In the APC$^{Min/+}$ colorectal cancer model, *F. nucleatum* potentiates intestinal tumorigenesis via a TLR4 signaling cascade (32). However, the link between *F. nucleatum*, OMVs, TLR4, and NF-κB activation in the noncancerous intestinal epithelium has not yet been fully addressed. Here, we connected these concepts and demonstrated that *F. nucleatum* produced OMVs activated TLR4 to drive extracellular signal-regulated kinase (ERK), CREB, NF-κB, and proinflammatory cytokines in human cell lines and human colonoid monolayers. We also identified a role for *F. nucleatum* in initiating colonic inflammation in mice harboring a human microbiome.

RESULTS

***F. nucleatum* subspecies *polymorphum* adheres to intestinal mucus and secretes OMVs.** Several studies have identified increased abundances of the oral microbe *Fusobacterium* in setting of colorectal cancer (29, 33–35), liver cirrhosis (36–38), primary sclerosing cholangitis (39–41), gastroesophageal reflux disease (42–46), HIV infection (47–49), alcoholism (50), and IBD (6, 10–19). Given the prevalence of *F. nucleatum* in mucosal specimens, we tested the hypothesis that this pathobiont could promote an epithelial proinflammatory response and potentially contribute to intestinal inflammation. Using fluorescently tagged *F. nucleatum* subsp. *polymorphum* ATCC 10953, we found that *F. nucleatum* resided in aggregates in the mucus layer adjacent to human colonic T84 cells (Fig. 1A). To confirm binding to the mucus layer, we also examined adhesion of *F. nucleatum* to coverslips coated with purified MUC2 from T84 cells and observed robust adhesion (Fig. 1B). Colonization of the intestinal mucus layer allows microbes such as *F. nucleatum* to secrete host-modulating subcellular structures or compounds in close proximity to the epithelium. One potential subcellular structure that could influence the host is the OMV. Previous groups have shown that *F. nucleatum* subsp. *nucleatum* and *F. nucleatum* subsp. *animalis* can secrete OMVs (31, 51). Consistent with these findings, we observed *F. nucleatum* subsp. *polymorphum*
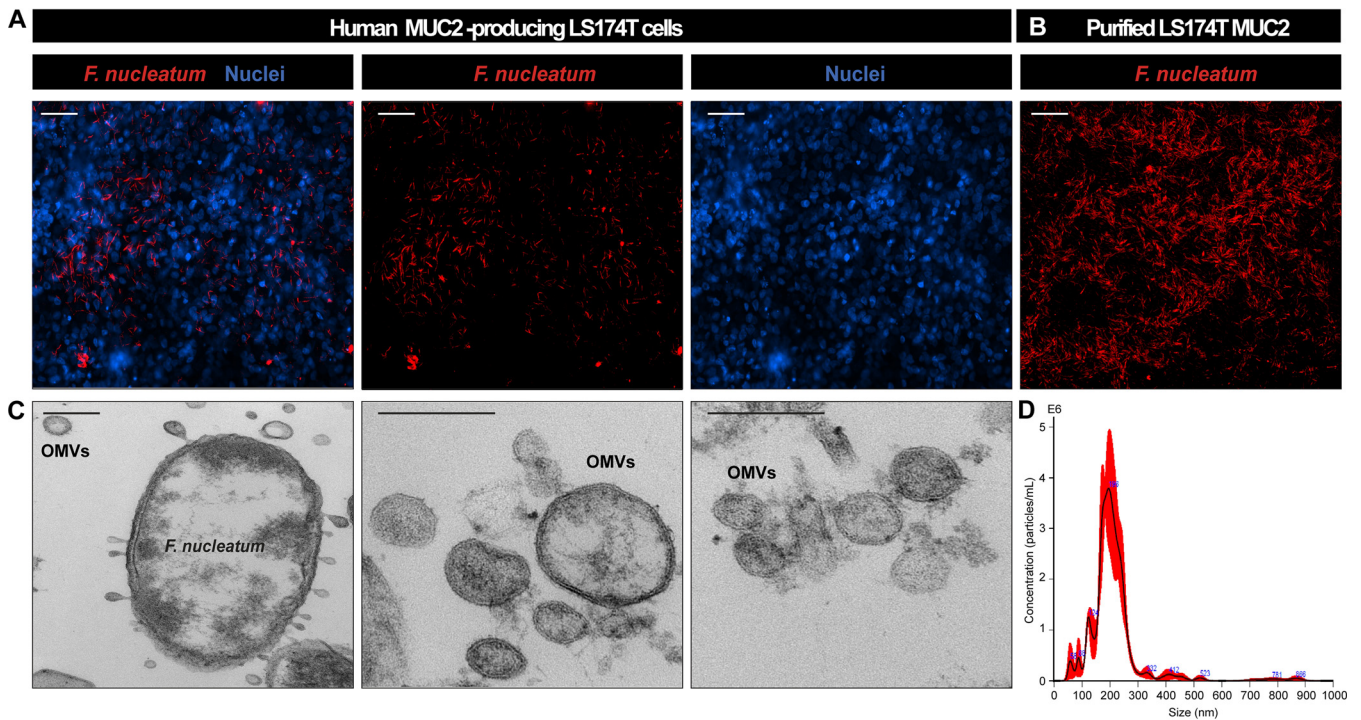
FIG 1 *F. nucleatum* subsp. *polymorphum* adheres to colonic MUC2 and secretes OMVs. (A) Representative images of T84 cells after incubation with fluorescently tagged *F. nucleatum* subsp. *polymorphum* counterstained with nuclear dye Hoechst (scale bar, 50 µm). (B) Representative image of fluorescently tagged *F. nucleatum* subsp. *polymorphum* adhered to purified MUC2 (scale bar, 50 µm). (C) TEM images of *F. nucleatum* (cross-section) with OMVs attached and surrounding the bacterium. Images on the right-hand side depict the various sizes of OMVs (scale bar, 200 nm). (D) Nanoparticle tracking analysis of *F. nucleatum* subsp. *polymorphum* OMVs.

secreted a range of OMVs, with an average hydrodynamic diameter of 212 ± 7 nm, as determined by NanoSight (Fig. 1C and D).

F. nucleatum subsp. polymorphum secreted compounds and purified OMVs promote secretion of colonic proinflammatory cytokines. OMVs from other Gram-negative species can activate innate immune responses, such as TLRs, which can activate the NF-κB pathway and drive proinflammatory cytokine responses (32). We hypothesized that *F. nucleatum* secreted virulence factors, such as OMVs, would promote proinflammatory effects in epithelial cells. To test this hypothesis, we cultured *F. nucleatum* subsp. *polymorphum* in BHIS (supplemented brain heart infusion medium) for 48 h and size-fractionated the supernatants to less than or greater than 50 kDa. The size-fractionated conditioned medium was applied to HT29 cell monolayers, and IL-8 production was measured to determine whether secreted factors from *F. nucleatum* stimulated a proinflammatory immune response. Conditioned medium fractions less than 50 kDa (<50 kDa) behaved similarly to the negative control (BHIS) and had no effect on IL-8 production by HT29 cells (Fig. 2A). However, the addition of conditioned medium fractions greater than 50 kDa (>50 kDa) containing particles above 2.4 nm, including OMVs, stimulated an ~9-fold increase in IL-8 secretion compared to medium alone. That addition of purified *F. nucleatum* OMVs to HT29 cell monolayers also stimulated IL-8 production, suggesting that the active secreted factors in the >50-kDa fraction of conditioned media included OMVs. Pretreatment of HT29 cells for 1 h with the TLR4 inhibitor CLI-095 significantly attenuated the secretion of IL-8 in response to >50-kDa *F. nucleatum* conditioned media and OMVs. This result suggested that TLR4 activation results in stimulation of IL-8 production by *F. nucleatum* subsp. *polymorphum*. A similar pattern was observed for TNF secretion (Fig. 2B); >50-kDa and purified *F. nucleatum* OMVs stimulated an ~6-fold increase in TNF secretion compared to uninoculated BHIS control and <50-kDa *F. nucleatum* conditioned media (Fig. 2B).
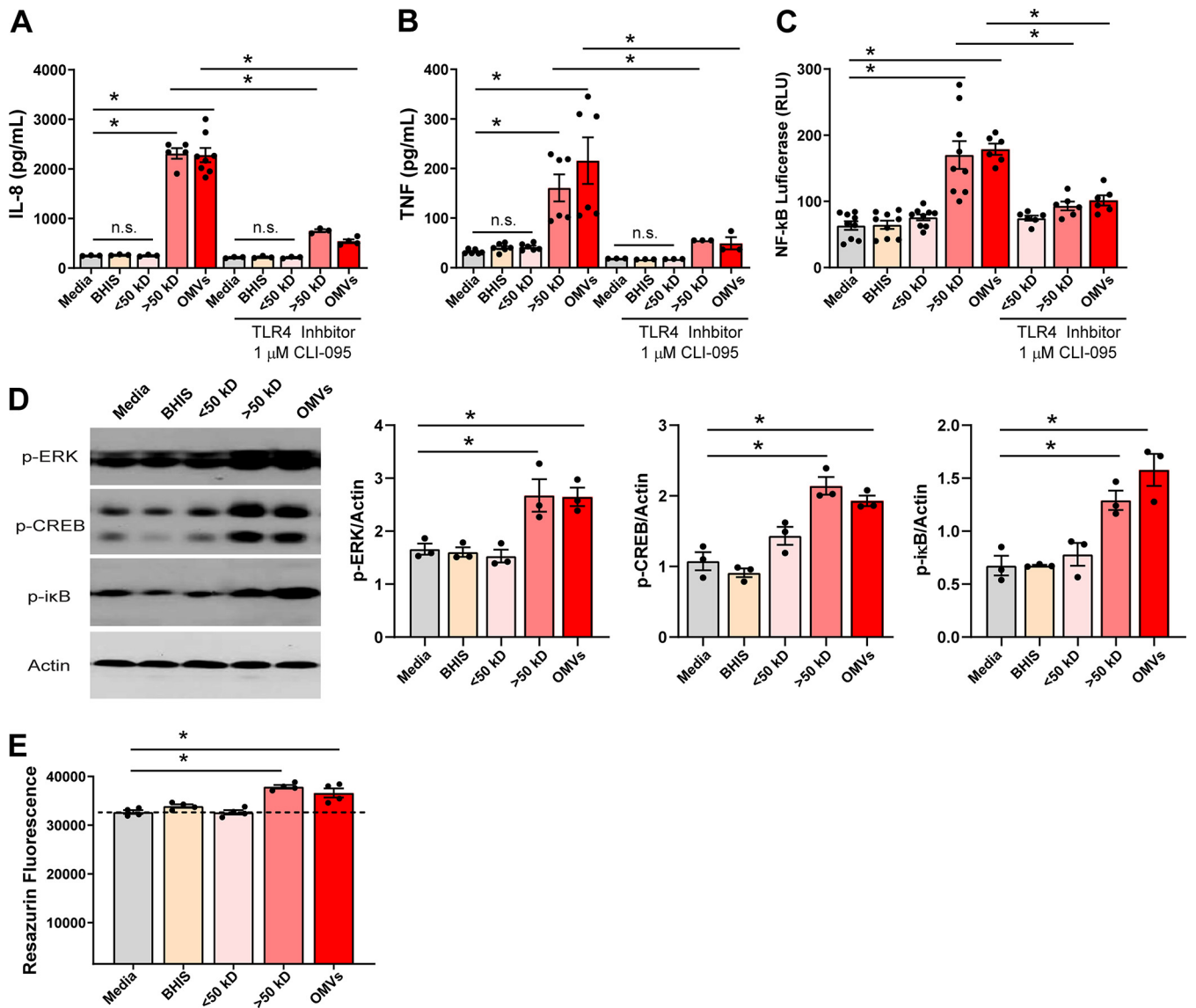
FIG 2 *F. nucleatum* compounds and OMVs promote IL-8, TNF, NF-κB, and MAPK activation. (A) Measurement of IL-8 (pg/ml) by ELISA in HT29 cell supernatant after 16 h of incubation with 25% uninoculated BHIS (BHIS), 25% *F. nucleatum* BHIS conditioned medium <50-kDa fraction (<50 kDa), 25% *F. nucleatum* BHIS conditioned medium >50-kDa fraction (>50 kDa), or 5% purified *F. nucleatum* OMVs (OMVs) in DMEM in the absence or presence of TLR4 inhibitor CLI-095 (*n* = 6 replicates/experiment, repeated three independent times). (B) Measurement of TNF (pg/ml) by ELISA in HT29 supernatant after 16 h incubation with 25% uninoculated BHIS (BHIS), 25% *F. nucleatum* BHIS conditioned medium <50-kDa fraction, 25% *F. nucleatum* BHIS conditioned medium >50-kDa fraction, or 5% purified *F. nucleatum* OMVs (OMVs) in DMEM in the absence or presence of TLR4 inhibitor CLI-095 (*n* = 6 replicates/experiment, repeated three independent times). (C) Quantification of secreted luciferase in HT29 cells transfected with a pNFκB-MetLuc2-Reporter treated for 16 h (*n* = 9/experiment, repeated two independent times). (D) Western blot analysis of phosphorylated ERK, phosphorylated CREB, phosphorylated iκB, total iκB, and actin at 30 min incubation in HT29 cells (*n* = 3/experiment). Treatments are the same as in panels A, B, and C. Quantification of Western blots was performed using Fiji software. (E) Analysis of metabolic activity/viability in HT29 cells by resazurin assay (excitation, 560; emission, 600 nm). *, $P < 0.05$ (multi-way ANOVA).

NF-κB is essential for upregulation of proinflammatory cytokines, including IL-8 (52). To assess whether NF-κB was activated by *F. nucleatum* secreted factors, we transfected HT29 monolayers with a pNFκB-MetLuc2-Reporter to monitor the activation of the NF-κB signal transduction pathway. Using this system, we observed a significant increase in secreted luciferase (indicating NF-κB activation) in response to the >50-kDa *F. nucleatum* conditioned media and purified OMVs compared to the medium control and <50-kDa *F. nucleatum* conditioned media (Fig. 2C). Incubation of HT29 cells with the TLR4 inhibitor resulted in an ~2-fold decrease in NF-κB luciferase production. Next, we examined additional downstream targets TLR4, ERK, and CREB by Western blotting after incubating HT29 cells with fractionated conditioned media or purified OMVs for

30 min (Fig. 2D). As expected, media control and the <50-kDa *F. nucleatum* conditioned media did not activate p-ERK p-CREB or p-iĸB at the 30-min time point. However, the addition of >50-kDa *F. nucleatum* conditioned media and purified OMVs increased the amounts of p-ERK, p-CREB, and p-iĸB compared to media control. Importantly, we did not observe a decrease in cell viability/metabolism. In fact, we observed a slight increase in the conversion of resazurin to resorufin, suggesting an increase in cell metabolism in response to *F. nucleatum* conditioned media (Fig. 2E). These data demonstrate a robust response of colonic epithelial cells to factors secreted by *F. nucleatum* subsp. *polymorphum*.

While HT29 colonic cancer-derived cells can model some intestinal epithelial functions, they do not reflect the intestinal epithelium as a whole (53). The human intestinal enteroid (HIE; also known as organoid) system has expanded our *in vitro* capabilities in understanding the physiology of the noncancerous human intestinal epithelium. HIEs are derived from intestinal stems cells and provide a long-term primary culture system. Importantly, HIEs harbor all cell lineages found in native tissue, are segment specific, and contain TLRs (53–55). We have previously shown that HIE media contains a number of antioxidants, including *N*-acetylcysteine, glutathione, B27 supplement, and N2 supplement, which dampen proinflammatory signaling cascades (54). However, by using a simplified media without anti-oxidants, we can generate HIEs that are responsive to microbial stimulation such as lipopolysaccharides (LPS), lipoteichoic acid, and flagellin. We used HIEs derived from colonic epithelial stem cells isolated from healthy adults to examine the effects of *F. nucleatum* secreted compounds on the uninflamed intestinal epithelium. Observation by light microscopy showed that treatment of colonic HIE monolayers with >50-kDa *F. nucleatum* conditioned media did not affect cell morphology (Fig. 3A). Treatment with the >50-kDa *F. nucleatum* conditioned media promoted TNF secretion by colonic HIE monolayers compared to the media control (Fig. 3B). In contrast to our HT29 model, we found no differences in IL-8 secretion between media control and *F. nucleatum* conditioned media (data not shown). Transfection of colonic HIE monolayers with the pNFĸB-MetLuc2-Reporter confirmed upregulation of NF-ĸB after treatment with *F. nucleatum* conditioned medium (Fig. 3C). Analysis of HIE cell lysates by Luminex Magpix revealed increased p-ERK and p-CREB after treatment with >50-kDa *F. nucleatum* conditioned media, consistent with our HT29 cell data. These data confirm our HT29 cell data and demonstrate that >50-kDa compounds produced by *F. nucleatum* can stimulate epithelial inflammatory signals.

F. nucleatum subsp. polymorphum promotes inflammation in a humanized mouse model following antibiotic administration. Based on our promising *in vitro* data, we next addressed whether *F. nucleatum* could elicit proinflammatory responses using a mouse model (Fig. 4). Since *Fusobacterium* spp. are commonly found in the gastrointestinal tracts of humans, but not mice (56), and may have unique interactions with human-derived microbes, we used mice colonized with a human intestinal microbiota, also known as humanized microbiota mice. Mice were orally gavaged with a single dose of *F. nucleatum* (10^9 CFU) and euthanized on day 3 and day 5 postinoculation with *F. nucleatum*. No changes were observed in the crypt architecture or immune infiltration of the intestinal epithelium from mice treated with *F. nucleatum* at days 3 or 5 postinoculation (Fig. 4A). Likewise, *F. nucleatum* was not identified in the colonic mucus layer by FISH (Fig. 4B), although low levels of *Fusobacterium* gDNA was found in the feces by quantitative PCR (qPCR) analysis (Table 1), and no weight differences were observed between groups (Fig. 4C). A closer examination of colonic gene expression revealed no changes in the proinflammatory cytokine gene expression of KC (the mouse homolog to IL-8), IL-6, IFN-γ, and monocyte chemoattractant protein-1 (MCP-1) in *F. nucleatum*-treated mice at days 3 or 5 when an intact gut microbiota was present (Fig. 4D and E). These findings suggest that *F. nucleatum* does not have detrimental effects on overall health parameters in the setting of an intact human microbiota.

We previously detected increased *Fusobacterium* operational taxonomic unit (OTU) abundance in stool samples from patients on antibiotics (57). As result, we reasoned
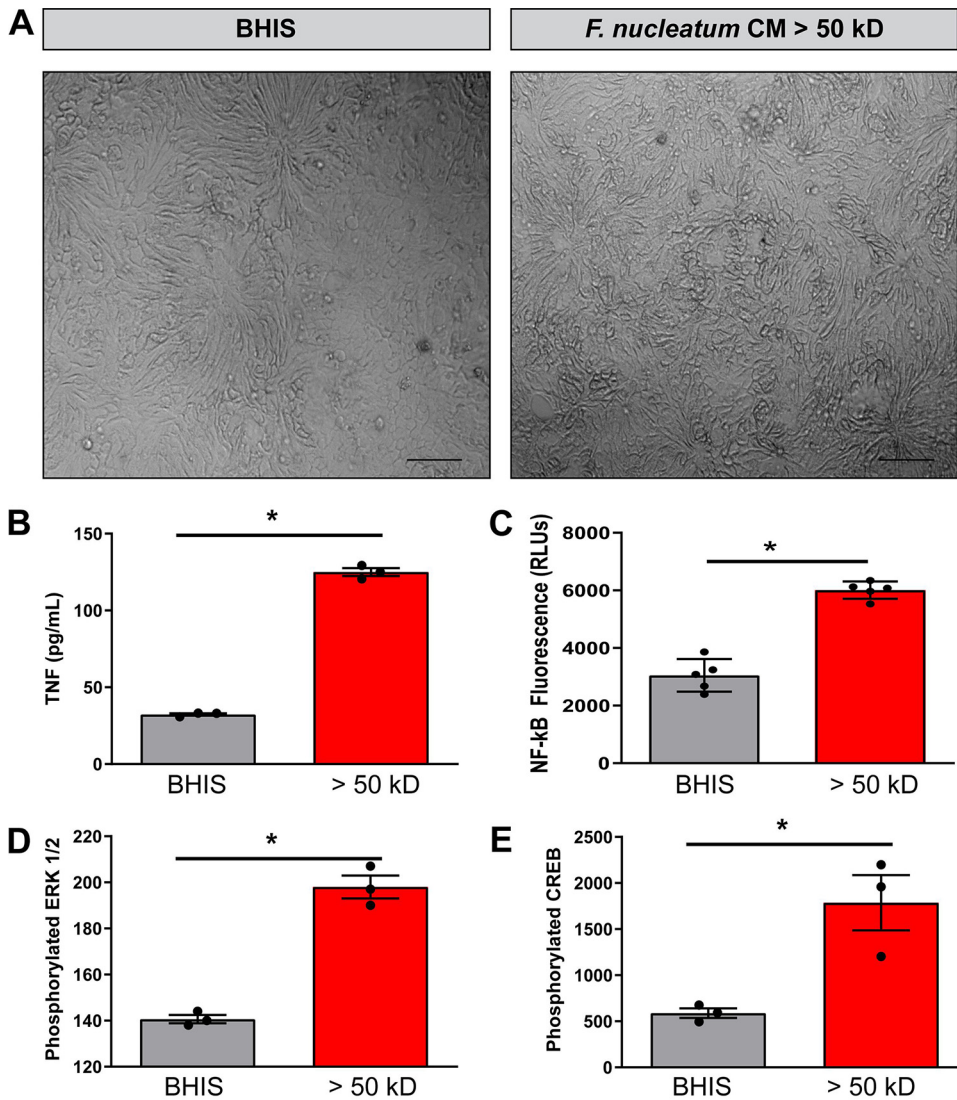
FIG 3 *F. nucleatum* >50-kDa compounds promote TNF, NF-κB, and MAPK signaling in human colonoid monolayers. (A) Representative images of human colonoid monolayers treated with 25% BHIS (BHIS) or 25% *F. nucleatum* conditioned medium >50-kDa fraction (>50 kDa) in DMEM, 1× HEPES, 1× GlutaMAX, and pyruvate for 16 h (scale bar,100 μm). (B) Measurement of TNF (pg/ml) by ELISA in colonoid monolayers treated with 25% BHIS (BHIS) or 25% *F. nucleatum* BHIS conditioned medium >50-kDa fraction after 16 h incubation ($n = 4$ monolayers/experiment, repeated two independent times). (C) Quantification of secreted luciferase in human colonoid monolayer cells transfected with a pNFκB-MetLuc2-Reporter treated for 16 h ($n = 4$ monolayers/experiment). (D and E) Luminex Magpix multiplex analysis of phosphorylated ERK (D) and CREB (E) in human colonoid monolayers treated with 25% BHIS (BHIS) or 25% *F. nucleatum* conditioned medium >50-kDa fraction for 1 h ($n = 3$ monolayers/experiment). *, $P < 0.05$ (Student t test).

that *F. nucleatum* may require an available niche to promote intestinal inflammation. To address this question, humanized microbiota mice were treated with a cocktail of antibiotics (kanamycin, gentamicin, colistin, metronidazole, and vancomycin) for 5 days, followed by a single injection of clindamycin. This broad-spectrum antibiotic regimen has previously been shown decrease multiple bacterial OTUs by 16S rRNA sequencing (58). Directly after antibiotic treatment, the mice were orally gavaged with *F. nucleatum* (10^9 CFU). This treatment regimen was designed to alter the microbiome and provide a potential niche for *F. nucleatum*. The intestinal epithelium from mice euthanized at day 3 postinoculation with *F. nucleatum* exhibited disruption of the colonic architecture, with increased immune infiltration and a depleted mucus layer which resulted in luminal contents being closer in proximity to the intestinal epithelium
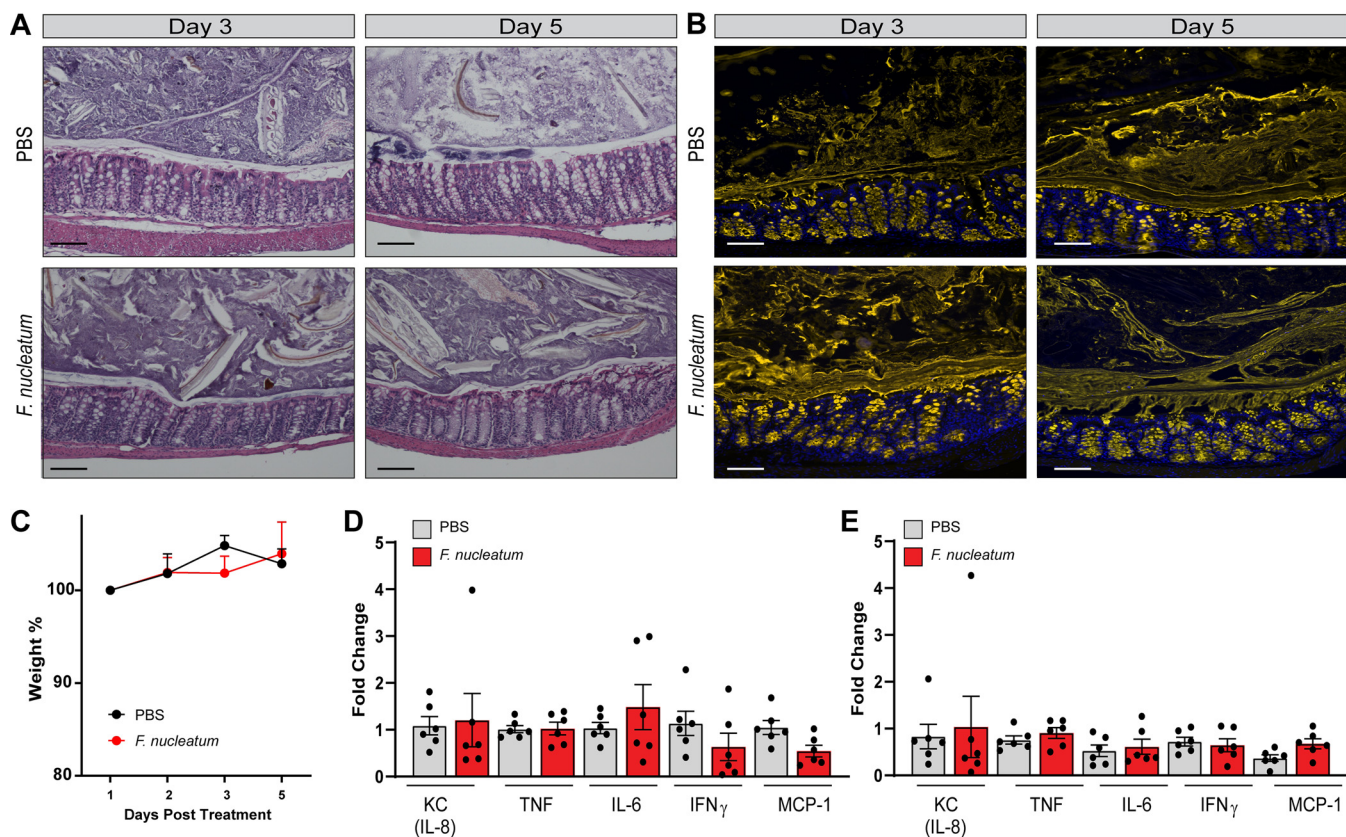
FIG 4 *F. nucleatum* subsp. *polymorphum* is unable to promote inflammation in the presence of a complete gut microbiome. (A) Representative images of H&E stains of control animals and *F. nucleatum* subsp. *polymorphum*-treated animals at day 3 and day 5 postinfection (scale bar, 100 µm). (B) FISH staining of *Fusobacterium* (red) counterstained with MUC2 (yellow) and Hoechst (blue) at day 3 and day 5 postinfection (scale bar, 100 µm). (C) Analysis of mouse weights at days 1, 2, 3, and 5 postinfection ($n = 6$/group). *, $P < 0.05$ (repeated-measures ANOVA). (D) Colonic mRNA expression of proinflammatory related genes on day 3 postinfection ($n = 6$/group). *, $P < 0.05$ (two-way ANOVA). (E) Colonic mRNA expression of proinflammatory related genes on day 5 postinfection ($n = 6$/group). *, $P < 0.05$ (two-way ANOVA).

(Fig. 5A). After 5 days postinoculation with *F. nucleatum*, colonic epithelia of mice exhibited reduced architecture disruption and immune infiltration compared to day 3, but still displayed loss of goblet cells and a thinner mucus layer. Fluorescence *in situ* hybridization (FISH) confirmed the presence of *F. nucleatum* in the epithelial mucus layer at both days 3 and 5, with the greatest numbers of bacteria observed at day 3 (Fig. 5B and Table 1). Oral gavage with *F. nucleatum* also correlated with weight loss compared to phosphate-buffered saline (PBS)-treated mice, supporting the notion that *F. nucleatum* had negative effects on health (Fig. 5C). Analysis of colonic gene expression revealed increased concentrations of epithelial- and immune-cell-secreted KC (the mouse IL-8 homologue) and immune-cell-secreted IL-6, IFN-γ, and MCP-1 in *F. nuclea-*

TABLE 1 Calculated *Fusobacterium* fecal load based on standard cultures of *F. nucleatum* subspecies *polymorphum*

Treatment	Mean *Fusobacterium* CFU ± SEM[a]	
	No Abx	Abx
Day 3		
PBS	0	0
F. nucleatum	$3.1 \times 10^1 \pm 0.6 \times 10^1$	$2.4 \times 10^4 \pm 1.5 \times 10^3$
Day 5		
PBS	0	0
F. nucleatum	0	$4.3 \times 10^3 \pm 0.8 \times 10^3$

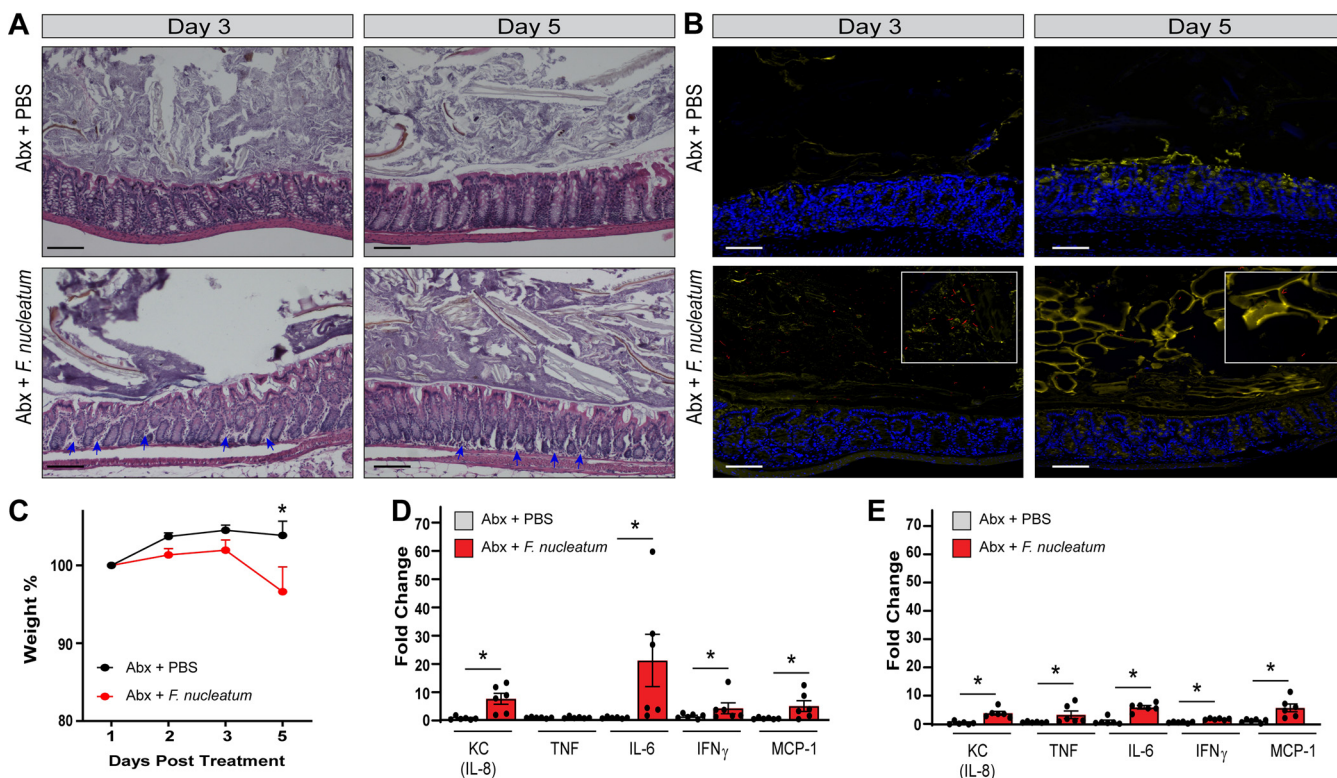[a]As determined by qPCR. Abx, antibiotics.

FIG 5 *F. nucleatum* subsp. *polymorphum* drives inflammation *in vivo* with antibiotic disruption of the gut microbiome. (A) Representative images of H&E stains of control animals and *F. nucleatum* subsp. *polymorphum*-treated animals who received antibiotics at day 3 and day 5 postinfection (scale bar, 100 μm). Blue arrows highlight immune infiltration. (B) FISH staining of *Fusobacterium* (red) counterstained with MUC2 (yellow) and Hoechst (blue) at day 3 and day 5 postinfection. Enlarged insets demonstrate *Fusobacterium* at day 3 and 5 (scale bar, 100 μm). (C) Analysis of mouse weights at days 1, 2, 3, and 5 postinfection (*n* = 6/group). *, *P* < 0.05 (repeated-measures ANOVA). (D) Colonic mRNA expression of proinflammatory related genes on day 3 postinfection (*n* = 6/group). *, *P* < 0.05 (two-way ANOVA). (E) Colonic mRNA expression of proinflammatory related genes on day 5 postinfection (*n* = 6/group). *, *P* < 0.05 (two-way ANOVA).

tum-treated mice compared to PBS treatment at day 3 (Fig. 5D). IL-6 showed the greatest change in increased expression at day 3 postinoculation with *F. nucleatum*. With the exception of TNF, cytokine gene expression was substantially lower in the *F. nucleatum* group on day 5 compared to that observed on day 3 (Fig. 5E). However, KC, TNF, IL-6, IFN-γ, and MCP-1 were still increased in the *F. nucleatum*-treated mice compared to mice gavaged with PBS control. These data indicate that *F. nucleatum* is capable of driving a proinflammatory signaling cascade *in vivo* in the presence of an antibiotic-disrupted humanized microbiota. Collectively, these findings expand our knowledge of *F. nucleatum*-host interactions and indicates that orally derived *F. nucleatum* can stimulate inflammatory responses.

DISCUSSION

Providing a deeper understanding of how *F. nucleatum* promotes inflammation could potentially lead to novel therapeutic approaches for the treatment of multiple intestinal diseases. Our data indicate that *F. nucleatum* subsp. *polymorphum* secretes OMVs, which can activate TLR4 and downstream targets ERK, CREB, and NF-κB, thereby promoting proinflammatory cytokine production. These effects were observed in colonic HT29 cells, as well as in human colonoid (organoid) monolayers. These *in vitro* data support the hypothesis that *F. nucleatum* is capable of eliciting intestinal inflammation through the production of secreted compounds, among other mechanisms. In mice harboring a human microbiome, we found that antibiotic treatment allowed *F. nucleatum* to adhere to the intestinal mucus layer and drive inflammation, as indicated by weight loss, increased immune infiltration,

altered colonic architecture, and proinflammatory cytokine mRNA signatures. We also found that antibiotic-mediated depletion of the gut microbiome is essential for *F. nucleatum*-mediated effects. These data provide solid evidence that *F. nucleatum* can promote inflammation in the gastrointestinal tract when an open niche is available.

The majority of research on *F. nucleatum* has focused on its role as a periodontal pathogen. However, in recent years investigators have begun to view *F. nucleatum* as an intestinal pathogen as well (11, 12). This is largely due to the identification of *F. nucleatum* in colonic biopsy specimens from patients with IBD and colorectal cancer (10, 11, 13, 14, 17, 29, 30, 35, 59–66). Many Gram-negative bacteria, including *F. nucleatum*, release OMVs both *in vitro* and *in vivo* (67–69), and these nanoparticles have been implicated as major players in bacterial pathogenesis. OMVs commonly contain LPS, DNA, adhesins, and enzymes and therefore have been proposed to act as a delivery system for these virulence factors (70). Our *in vitro* work indicates the TLR4 activation by *F. nucleatum*-conditioned media, including OMVs, play a significant role in epithelial cytokine production. As a result, we speculate that outer membrane LPS may be driving this effect. Consistent with this hypothesis, we observed that application of purified LPS from *F. nucleatum* subsp. *polymorphum* also stimulated IL-8 in our HT29 cells (data not shown). However, we do not think that TLR4 is the only pathway employed by *F. nucleatum* secreted compounds and OMVs. In colon cancer studies, *F. nucleatum* stimulation of proinflammatory cytokines was found to occur by both TLR4-dependent and -independent mechanisms (71). Park et al. demonstrated that *F. nucleatum* activates both TLR2 and TLR4 in bone-marrow-derived macrophages to stimulate IL-6 production (72), an effect that is completely ablated in the absence of MyD88. Thus, it is likely that other TLRs may be activated in response to *F. nucleatum*-secreted products. As a result, we speculate that OMVs activate epithelial cells and immune cells through both TLR4-dependent and -independent mechanisms *in vivo*. We speculate that, similar to cancer models, inflammation associated with *F. nucleatum* is likely dependent on MyD88 signaling. In addition to LPS, there are many proteins in *F. nucleatum* OMVs with potential virulence functions. These proteins include FomA, FadA, FadD, Fad-I, NapA, ClpB, GroEL, TraT, and YadA; future studies on their contributions to disease are needed.

In addition to OMVs, *F. nucleatum* may secrete other compounds which stimulate TLRs and drive inflammation. Although our *in vitro* studies suggest that OMVs contribute to inflammation, it is possible that our >50-kDa fraction also contains other large-molecular-weight compounds capable of stimulating cytokines. In addition, it is possible that large-molecular-weight compounds act in synergy with OMVs to drive inflammation. Our *in vivo* studies do not exclude other mechanisms of inflammation. Future studies are warranted to address the role of other factors in stimulating inflammatory signals.

In addition to secreted factors, several studies have found that *F. nucleatum* is capable of invading epithelial cells and can directly activate proinflammatory signals (73–75). *F. nucleatum* invasion of oral epithelial cells activates NF-κB and induces proinflammatory cytokines (IL-8, TNF, IL-1β, and IL-6) (73–75). In the setting of cancer, *F. nucleatum* invasion of cancer cells also induces NF-κB and proinflammatory cytokine production (11, 29, 30, 35, 62, 64, 71). Although we observed cytokine production and inflammation in our studies, we saw little evidence of epithelial invasion by *F. nucleatum* by our FISH staining. We found that *F. nucleatum* can adhere to colonic mucin glycans and predict mucus adhesion may limit the invasion of *F. nucleatum* into the epithelium. Another possible explanation of the lack of invasion may be explained by the intact epithelium in our mouse model. It is possible that *F. nucleatum* may require damage or epithelial fragility to invade the colonic epithelium. In addition, our findings may be strain dependent, since clinical isolates from patients with IBD have been characterized to be more proinflammatory than *F. nucleatum* isolated from healthy subjects. For example, *F. nucleatum* isolated from inflamed regions of the gut exhibit

enhanced invasion of Caco-2 cells and trigger TNF (76). These results suggest that although *F. nucleatum* may be proinflammatory in general, some strains are more pathogenic than others.

Our data indicate that *F. nucleatum* requires disruption of the microbiome to promote inflammation. Previous work from Collins et al. using the same humanized mouse model demonstrated that antibiotic treatment significantly reduced the levels of *Lachnospiraceae*, *Bacteroidaceae*, *Clostridiaceae*, and *Verrucomicrobiaceae* compared to mice without antibiotics (58). These findings appear to resemble that of microbial composition in intestinal microbiomes of patients in IBD, both ulcerative colitis (UC) and Crohn's disease (CD), whereas a diminution of *Lachnospiraceae* and *Bacteroidetes* has been observed compared to healthy volunteers or non-IBD controls (77–80). In addition, the gut microbiota of the patients with colorectal cancer are often depleted in *Lachnospiraceae*, *Bacteroidetes*, and *Clostridia* and enriched in *Fusobacterium* (65, 81–85). One study identified that high abundance of *Lachnospiraceae* was negatively associated with the colonization of colonic tissue by oral microbes (*Fusobacterium*, *Streptococcus*, *Gemella*, etc.) (84). These microbiome studies suggest a protective colonization resistance role for select gut microbes, such as *Lachnospiraceae* and commensal *Bacteroides*. We theorize that the presence of *Lachnospiraceae*, *Bacteroidetes*, and other antibiotic-depleted microbes may prevent *F. nucleatum* colonization and therefore inflammation.

The intestinal microbiome is resilient and can revert back toward the original population following antibiotic treatment. Consistent with this notion, Collins et al. observed resolution of the microbiome in the same human microbiome mouse model following antibiotics and predicted that the microbial communities would eventually return to baseline (58). As a result, we speculate that *F. nucleatum* subsp. *polymorphum* would not persist in our antibiotic-treated mouse model long term. We predict that as the microbiome returned, *F. nucleatum* would be outcompeted, and there would be resolution of inflammation. By day 5 postgavage, we observed less *F. nucleatum* by FISH staining and lower inflammatory markers in the antibiotic-treated mice compared to day 3. We predict that the effects of *F. nucleatum* would only remain for a few more days (ca. days 7 to 10) as the microbiome returned to its usual complexity. To fully address this question, more studies are needed to determine the precise balance of *F. nucleatum* and the microbiome following antibiotic administration.

Fusobacterium is commonly found in mixed microbial infections (86). This is due in part to the communal nature of *F. nucleatum*. It harbors multiple adhesins which promote multispecies biofilm formation (87–92). These microbe-microbe interactions have been well documented in the oral cavity; however, biofilm formation may also be a potential strategy for *F. nucleatum* colonization in the gut. It is possible that the microbes present after antibiotics interact with *F. nucleatum* and promote its persistence. Since oral microbes are commonly found in intestinal disease states and *F. nucleatum* is known to aggregate and form biofilms with multiple oral bacteria (87–91, 93–97), a synergy may exist between these groups to promote intestinal inflammation and pathology. Ledder et al. demonstrated that *F. nucleatum* can coaggregate with intestinal microbes, including *Bifidobacterium adolescentis* and *Lactobacillus paracasei*, and to a lesser degree with *Bacteroides vulgatus* and *Enterococcus faecium* (91). Therefore, *F. nucleatum* may be interacting with mucosa-associated gut microbes to enhance colonization.

Overall, our findings indicate that *F. nucleatum* can promote inflammation in normal epithelial cells *in vitro* and *in vivo* (Fig. 6). We speculate that certain strains of *F. nucleatum* in genetically susceptible patients may be an initiating or contributing factor to inflammation. We predict that in patients undergoing antibiotics, the microbiome does not provide colonization resistance and *F. nucleatum* can establish residence. We also reason that an aberrant immune response coupled with an altered microbiome and *F. nucleatum* could lead to chronic inflammation. As a result, our findings point to *F.*
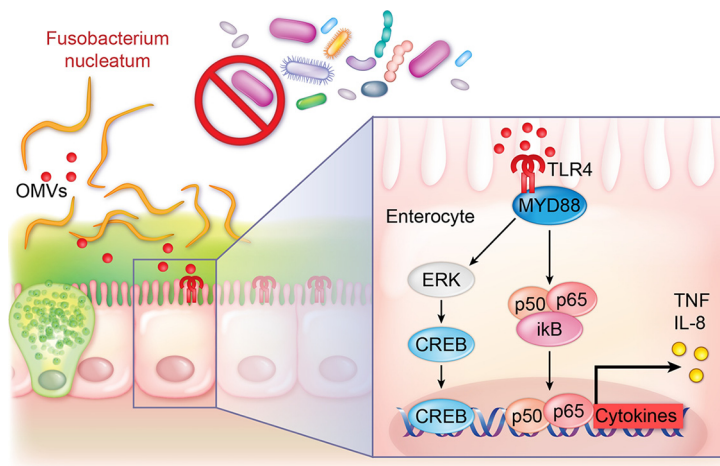
FIG 6 Proposed model for *F. nucleatum* subsp. *polymorphum*-driven inflammation. *F. nucleatum* adheres the intestinal mucus layer in the setting of an altered gut microbiome, in which it delivers secreted compounds as "cargo" in OMVs. The OMVs activate epithelial TLRs, including TLR4, which promotes phosphorylation and activation of ERK, CREB, and NF-κB, thereby driving the production of proinflammatory cytokines and initiating inflammation.

nucleatum and OMVs as drivers of intestinal inflammation and warrant further study as future targets for treatment strategies aimed at reducing mucosal inflammation.

MATERIALS AND METHODS

Bacterial culture conditions. *Fusobacterium nucleatum* subsp. *polymorphum* ATCC 10953 (American Type Culture Collection) was cultured in brain heart infusion medium (Difco) supplemented with 2% yeast extract and 0.2% cysteine (BHIS) anaerobically at 37°C in an anaerobic workstation (Anaerobe Systems AS-580) with a mixture of 5% CO_2, 5% H_2, and 90% N_2.

(i) Preparation of *F. nucleatum* subsp. *polymorphum* conditioned media. To assay compounds secreted by *F. nucleatum*, we prepared conditioned media as follows. Overnight cultures were subcultured into BHIS at an optical density at 600 nm (OD_{600}) of 0.1 and cultured anaerobically for 48 h at 37°C. Cells were centrifuged at 7,000 × g for 5 min, and the supernatant was filter sterilized using 0.45-μm polyvinylidene difluoride Millipore centrifuge filters. This filtered supernatant was termed conditioned media (CM). *F. nucleatum* CM was size fractionated with Amicon Ultra 50-kDa centrifugal filters (Millipore, UFC905024). The fraction below 50 kDa was termed "<50 kDa" and the fraction above 50 kDa was termed ">50 kDa."

(ii) Isolation of *F. nucleatum* subsp. *polymorphum* outer membrane vesicles. We isolated OMVs produced by *F. nucleatum* subsp. *polymorphum* as follows. BHIS medium (500 ml) was inoculated to an OD_{600} of 0.1 using *F. nucleatum* overnight cultures and incubated anaerobically at 37°C for 48 h. Cells were pelleted by centrifugation at 7,000 × g for 10 min. Cell-free supernatant was collected, mixed with 120 g of ammonium sulfate, and then incubated for 2 h at 4°C. The vesicle-containing precipitate was collected by centrifugation at 10,000 × g for 20 min, and the pellets resuspended in 50 mM HEPES buffer (pH 7.5). The resuspended pellets were dialyzed overnight in 50 mM HEPES (pH 7.5) buffer at 4°C using 10,000-molecular-weight cutoff dialysis tubing. The vesicles were concentrated with >50-kDa Amicon Ultra centrifugation filters and added to OptiPrep solution (Sigma, D1556) at a ratio of 1:3 (vol/vol). This suspension was then added to 45% OptiPrep in Ultraclear centrifuge tubes and ultracentrifuged at 292,700 × g (70 Ti rotor; Beckman Coulter Inc.) for 3 h. Sequential fractions were collected and analyzed by 15% SDS-PAGE to identify fractions containing vesicles. Vesicle-containing fractions were pooled, diluted 10-fold in DPBS (Thermo Fisher, catalog no. 14190144), and separated from the OptiPrep by centrifugation at 38,400 × g for 3 h to remove the OptiPrep solution. Finally, the purified OMVs were resuspended in 500 μl of DPBS and used for microscopy and tissue culture experiments.

(iii) OMV analysis measured by NTA. Nanoparticle tracking analysis (NTA) was performed to determine the size of the OMVs using a NanoSight LM10 instrument (Malvern, Westborough, MA). Equipped with a sample chamber, a laser light source of 532 nm, sCMOS camera, and an optical microscope. The samples were diluted by 200-fold in Millipore water and the particle concentration were between 1.2E+8 to 4.0E+8 particles/ml. The samples were injected into the LM10 unit with a 1-ml syringe at a syringe pump speed of 100. The capturing settings (camera level, slider shutter, and gain) were adjusted automatically. The NanoSight LM10 recorded 30-s sample videos, which were analyzed by using NTA3.4 software. The particle diameter was obtained from the Stokes-Einstein equation.

(iv) Fluorescent labeling of *F. nucleatum* subsp. *polymorphum*. Fluorescently tagged *F. nucleatum* subsp. *polymorphum* were generated by incubation with 10 μM carboxyfluorescein diacetate succinimidyl ester (CFDA-SE) as previously described (98). Briefly, *F. nucleatum* subsp. *polymorphum* was grown

overnight in BHIS anaerobically at 37°C. The following day, the cultures were centrifuged at 5,000 × g for 5 min, and the pellet was washed twice with anaerobic PBS. *F. nucleatum* was then incubated with 10 μM CFDA-SE (Thermo Fisher, C1157) in PBS anaerobically at 37°C for 1 h. After incubation, CFDA-SE tagged cultures were centrifuged at 5,000 × g for 5 min, and the pellet was washed three times with anaerobic PBS to remove the residual CFDA-SE. Fluorescence was confirmed by microscopy.

Tissue culture. *In vitro* experiments were performed with the human colon cell line HT-29 (ATCC HTB-38). HT29 cells were maintained in McCoy's 5A medium (ATCC) supplemented with heat-inactivated 10% fetal bovine serum (FBS; Invitrogen) and antibiotics (100 U/ml penicillin and 100 μg/ml streptomycin) at 37°C and 5% CO_2. For adhesion assays, the mucin-producing human colon T84 line (ATCC CL-248) was used. T84 cells were grown in Dulbecco modified Eagle medium (DMEM; Thermo Fisher) supplemented with 10% FBS in a humidified atmosphere at 37°C and 5% CO_2. Purified MUC2 was isolated from T84 cells and adhered to glass coverslips as previously described (99). For monolayer adhesion, T84 cells were seeded at 5 × 10^5 cells/well in a 24-well plate containing poly-L-lysine-coated glass coverslips and grown to confluence. Prior to adhesion assays, T84-coated coverslips were incubated with Hoechst 33342 (Invitrogen, H3570) for 10 min at room temperature to stain the epithelial nuclei. Fluorescently tagged *F. nucleatum* subsp. *polymorphum* was added to either T84 monolayers or APTS-coated MUC2-coated coverslips and incubated for 1 h at 37°C and 5% CO_2. After incubation, coverslips were washed three times with PBS and fixed with Clarke's fixative to preserve the mucus layer, and mounted coverslips were examined by microscopy.

To examine cytokine production, HT29 cells were seeded at 1 × 10^4 cells/well in 96-well tissue culture-treated plates (Corning) and incubated at 37°C and 5% CO_2 overnight. The following day, the cells were treated with either DMEM (without FBS or media), 25% uninoculated BHIS media in DMEM (BHIS), 25% *F. nucleatum* conditioned medium (<50-kDa fraction) in DMEM, 25% *F. nucleatum* conditioned medium (>50-kDa fraction) in DMEM, or 5% *F. nucleatum* OMVs in DMEM and then incubated overnight at 37°C and 5% CO_2. To examine the contribution of TLR4 to cytokine production, HT29 cells in 96-well plates were pretreated for 1 h with 1 μM CLI-095 (TLR4 inhibitor; InvivoGen, TLRLCLI95) and maintained in 1 μM CLI-095 throughout an overnight incubation. Supernatants were examined for IL-8 production by IL-8/CXCL8 DuoSet ELISA (R&D Systems, DY208-05) and TNF production by TNF-α DuoSet ELISA (R&D Systems, DY210-05). Cell viability/metabolism was confirmed by using the dye resazurin (7-hydroxy-3H-phenoxazin-3-one 10-oxide; Sigma, R7017) at a final concentration of 44 μM. Cells were incubated for 3 h at 37°C and 5% CO_2, and the fluorescence resulting from resazurin reduction to resorufin was analyzed using a microplate spectrofluorometer at an excitation wavelength of 570 nm and an emission wavelength of 600 nm.

For Western blot analysis, HT29 cells were seeded at 2 × 10^5 cells/well in 24-well tissue culture treated plates (Corning). After growing cells to confluence, the monolayers were treated as described for the 96-well plate assay (DMEM, 25% BHIS, 25% <50 kDa, 25% >50 kDa, and 5% OMVs) in DMEM (no FBS) for 30 min. Cells were then lysed with radioimmunoprecipitation assay buffer (Thermo Fisher Scientific, Waltham, MA) containing a protease inhibitor cocktail (Roche). After centrifugation, the protein concentrations were quantitated by a Bradford assay (100). Portions (50 μg) of total protein were resolved by SDS-PAGE and transferred to polyvinylidene difluoride (PVDF) membranes (Millipore, Billerica, MA). After a blocking step with 5% milk in PBS-Tween 20 (PBS-T) for 30 min at room temperature, the PVDF membranes were incubated at 4°C overnight with antibodies for phosphorylated ERK, CREB, and iκBα, as well as total iκBα and β-actin. After three washes with TBS-T, the PVDF membranes were incubated with horseradish peroxidase-conjugated secondary antibodies for 1 h at room temperature. After TBS-T washes, the membranes were developed with ECL substrate (GE Healthcare, Buckinghamshire, UK). Western blots were analyzed using Fiji (formerly ImageJ) software (National Institutes of Health).

To examine NF-κB activation, HT29 monolayers were grown to 75% confluence and transiently transfected with a NF-κB secreted luciferase reporter (Clontech, pNFκB-MetLuc2-Reporter) in Opti-MEM (Thermo Fisher) using the XtremeGene HP DNA transfection reagent (Roche) (101) at a final concentration of 0.6 μl of XtremeGene HP and 0.3 μg of DNA per well. HT29 monolayers were incubated for 48 h at 37°C and 5% CO_2. After transfection, the cells were treated with DMEM, 25% BHIS, 25% <50 kDa, 25% >50 kDa, and 5% OMVs) in DMEM (no FBS) for 16 h. The supernatants were examined for luciferase activity using a Lonza Lucetta tube luminometer.

Human colonoid cultures. The human stem cell-derived colonoid line C103 was purchased from the Baylor College of Medicine GEMs enteroid core. Three-dimensional human colonoids were cultured in complete medium with growth factors (CMGF+) in phenol red-free, growth factor-reduced Matrigel (Corning) as previously described (102–104). Colonoids at passage 9 were seeded into flat 96-well plates as described previously (104–109). Briefly, three-dimensional colonoids were dislodged from Matrigel domes, washed with an ice-cold solution of 0.5 mM EDTA in 1× PBS, and dissociated at 37°C for 4 min with 0.05% trypsin and 0.5 mM EDTA. After 4 min, the trypsin was inactivated with Advanced DMEM/F-12, 1× GlutaMAX, and 1× HEPES continuing 10% FBS. The dissociated colonoids were filtered through a 40-μm nylon cell strainer (Falcon, catalog no. 352340) to generate single cells and then suspended with CMGF+ and 10 μM Y-27632 Rock inhibitor. The solution was added to Matrigel-precoated 96-well plates, followed by incubation for 48 h at 37°C and 5% CO_2. After 48 h, the medium was changed to differentiation medium, which contains the same components as CMGF+ but without Wnt3A conditioned medium, R-spondin conditioned medium, SB202190, and nicotinamide and only 5% (vol/vol) Noggin conditioned medium, but still supplemented with 10 μM Y-27632 Rock inhibitor. The differentiation medium was changed daily for 5 days.

To examine *F. nucleatum* stimulation of colonoid monolayers, the differentiation medium was

changed to DMEM supplemented with 1× HEPES, 1× GlutaMAX, and 1× pyruvate. This simplified media has previously been demonstrated to improve cytokine production by human colonoids (54). Colonoids were treated with either 25% uninoculated BHIS or 25% *F. nucleatum* conditioned media (>50 kDa) in DMEM/HEPES/GlutaMAX/pyruvate media. For cytokine analysis, colonoids were treated for 16 h, and the supernatants were examined for IL-8 and TNF by ELISA. In order to examine NF-κB activation, 96-well colonoid monolayers were transduced on day 3 with NF-κB secreted luciferase reporter (Clontech, pNFκB-MetLuc2-Reporter) and incubated for an additional 2 days in differentiation media. After 16 h incubation with either 25% uninoculated BHIS or 25% >50 kDa, the supernatants were examined for secreted luciferase as described above. For intracellular signaling analysis, colonoid monolayers were treated for 1 h, washed with PBS containing Ca^{2+} and Mg^{2+}, lysed with Luminex lysis buffer, and analyzed with a Milliplex MAP multi-pathway total magnetic bead assay (Millipore, catalog no. 48-681-MAG) with a Magpix instrument (Luminex Corporation, Austin, TX). Magpix analysis was performed by the Functional Genomics and Microbiome Core of the Texas Medical Center Digestive Diseases Center. Data were collected and analyzed by using Luminex xPONENT for MAGPIX, version 4.2, build 1324, and Milliplex Analyst version 5.1.0.0, standard build 10/27/2012.

Animal models. Animal experiments were approved by the Institutional Animal Care and Use Committee (IACUC) at Baylor College of Medicine. For animal experiments, *F. nucleatum* subsp. *polymorphum* was cultured overnight anaerobically in BHIS and centrifuged at 7,000 × *g* for 5 min. The bacterial pellet was washed twice, with sterile anaerobic PBS viability confirmed by serial plating *F. nucleatum* on BHIS agar to calculate the CFU; the cells were adjusted to 10^9 cells ml^{-1} and used to treat animals as described below. Humanized microbiota C57BL/6 mice were generated as described previously (58) and maintained in a BCM BSL-2-approved animal facility. Adult mice (10 to 16 weeks) were administered an antibiotic cocktail (kanamycin [0.4 mg ml^{-1}], gentamicin [0.035 mg ml^{-1}], colistin [850 U ml^{-1}], metronidazole [0.215 mg ml^{-1}], and vancomycin [0.045 mg ml^{-1}]) *ad libitum* in drinking water for 3 to 5 days as previously described (58). After 24 h, the mice were treated with clindamycin (10 mg kg^{-1}, injected intraperitoneally). Mice were gavaged orally with sterile PBS (control) or *F. nucleatum* subsp. *polymorphum* in PBS (10^9 CFU) 24 h later. Mice were monitored twice daily and euthanized on day 3 and day 5 after oral gavage. No visual or behavioral differences were noted in mice receiving antibiotics compared to control mice (no antibiotic). To examine the contribution of the microbiome on *F. nucleatum*-induced inflammation, a subset of mice did not receive any antibiotic treatment and only received PBS (control) or *F. nucleatum* subsp. *polymorphum* in PBS (10^9 CFU). For all experiments, groups contained equal numbers of male and female mice to exclude sex bias (6 females/6 males per treatment group).

Intestinal tissue staining. (i) H&E and PAS-AB. Mouse colons were placed intact in cassettes and fixed in 10% Carnoy's fixative. Paraffin-embedded tissue sections (7 µm) were processed for hematoxylin and eosin (H&E) or periodic acid-Schiff/Alcian blue (PAS-AB) staining. H&E and PAS-AB sections were examined by bright-field and imaged on the Nikon Eclipse 90i (Nikon) microscope using a DS-Fi1-U2 camera (Nikon) with a differential interference contrast (DIC) objective.

(ii) Immunofluorescence. *F. nucleatum* localization was examined using a *Fusobacterium*-specific FISH probe (5′-CGCAATACAGAGTTGAGCCCTGC-3′), and total bacteria were examined using a universal bacterial FISH probe EUB338 (5′-GCTGCCTCCCGTAGGAGT-3′; Integrated DNA Technologies [IDT]) (110). Briefly, tissue sections were dehydrated and incubated with the *Fusobacterium* probe at 45°C in a dark humidifying chamber, hybridized for 45 min, and counterstained with MUC2 (1:200 dilution; Cloud-Clone Corp., PAA705Mu01) and Hoechst 33342 (Invitrogen, H3570). Immunostained slides were imaged on an Eclipse 90i (Nikon, Tokyo, Japan) with a 20× Plan Apo (NA 0.75) DIC objective, and the images were recorded using a CoolSNAP HQ2 camera (Photometrics) using a Nikon Intensilight C-HGFI mercury lamp.

Transmission electron microscopy of OMVs. *F. nucleatum* and OMVs were prepared for transmission electron microscopy (TEM) by fixing in 2.5% glutaraldehyde in 0.1 M cacodylate buffer at room temperature for 1 h, followed by further fixation at 4°C. Samples were postfixed in 1% tannic acid for 1 h, followed by 1% osmium tetroxide for 1 h and en bloc stained with 1% uranyl acetate. The samples were dehydrated with a graded ethanol series. Samples were infiltrated into Quetol-Spurrs resin using propylene oxide as a transition solvent and polymerized at 60°C for 48 h, as previously described (111). The resulting blocks were sectioned at 70 nm on 300-mesh copper grids and imaged on a Tecnai T12 transmission electron microscope at 100 kV using an AMT CMOS camera. OMV sizes were measured using Fiji software (NIH) from TEM images.

RNA isolation, gDNA isolation, and qPCR. RNA was extracted from mouse colons using TRIzol according to manufacturer details (Thermo Fisher, catalog no. 15596018). RNA (1 µg) was converted to cDNA using the SensiFAST cDNA synthesis kit (Bioline USA, Inc.) and examined by quantitative real-time PCR (qPCR). qPCR was accomplished on a QuantStudio 3 qPCR machine (Applied Biosystems) using FastSYBR Green (Thermo Fisher) and 10 nM concentrations of primers designed using PrimerDesign (Thermo Fisher). The relative fold change was calculated with the 18S rRNA housekeeping gene using the $\Delta\Delta C_T$ method.

gDNA was extracted from mouse stool using the Zymo gDNA isolation kit (Zymo) according to the manufacturer's instructors with the addition of two rounds of bead beating. To generate a standard curve for comparison, *F. nucleatum* was grown overnight in BHIS, and 1 ml was serial diluted and used to isolated gDNA. These same cultures were plated for CFU counts, generating matching gDNA and CFU values. gDNA from mouse stool and culture standards were examined using FAST SYBR green and primers (*Fusobacterium* forward, CAACCATTACTTTAACTCTACCATGTTCA; *Fusobacterium* reverse, GTTGACTT TACAGAAGGAGATTATGTAAAAATC) on a QuantStudio3 qPCR machine. The *Fusobacterium* load was

calculated based on the cycle of threshold (C_T) values of the standards and back-calculated to CFU by using a four-parameter logistics curve as previously described (112).

Statistics. Data are presented as means ± the standard deviations, with points representing individual mice. Comparisons between groups were made with the Student t test or one- or two-way analysis of variance (ANOVA), using the Holm-Sidak *post hoc* test. GraphPad was used to generate graphs and statistics (GraphPad Software, Inc., La Jolla, CA). A P value of <0.05 was considered significant, and "n" indicates the number of experiments performed.

REFERENCES

1. Gao L, Xu T, Huang G, Jiang S, Gu Y, Chen F. 2018. Oral microbiomes: more and more importance in oral cavity and whole body. Protein Cell 9:488–500. https://doi.org/10.1007/s13238-018-0548-1.
2. Atarashi K, Suda W, Luo C, Kawaguchi T, Motoo I, Narushima S, Kiguchi Y, Yasuma K, Watanabe E, Tanoue T, Thaiss CA, Sato M, Toyooka K, Said HS, Yamagami H, Rice SA, Gevers D, Johnson RC, Segre JA, Chen K, Kolls JK, Elinav E, Morita H, Xavier RJ, Hattori M, Honda K. 2017. Ectopic colonization of oral bacteria in the intestine drives TH1 cell induction and inflammation. Science 358:359–365. https://doi.org/10.1126/science.aan4526.
3. Schmidt TS, Hayward MR, Coelho LP, Li SS, Costea PI, Voigt AY, Wirbel J, Maistrenko OM, Alves RJ, Bergsten E, de Beaufort C, Sobhani I, Heintz-Buschart A, Sunagawa S, Zeller G, Wilmes P, Bork P. 2019. Extensive transmission of microbes along the gastrointestinal tract. Elife 8. https://doi.org/10.7554/eLife.42693.
4. Inohara N. 2017. Route connection: mouth to intestine in colitis. Cell Host Microbe 22:730–731. https://doi.org/10.1016/j.chom.2017.11.012.
5. Olsen I, Yamazaki K. 2019. Can oral bacteria affect the microbiome of the gut? J Oral Microbiol 11:1586422. https://doi.org/10.1080/20002297.2019.1586422.
6. Gevers D, Kugathasan S, Denson LA, Vazquez-Baeza Y, Van Treuren W, Ren B, Schwager E, Knights D, Song SJ, Yassour M, Morgan XC, Kostic AD, Luo C, Gonzalez A, McDonald D, Haberman Y, Walters T, Baker S, Rosh J, Stephens M, Heyman M, Markowitz J, Baldassano R, Griffiths A, Sylvester F, Mack D, Kim S, Crandall W, Hyams J, Huttenhower C, Knight R, Xavier RJ. 2014. The treatment-naive microbiome in new-onset Crohn's disease. Cell Host Microbe 15:382–392. https://doi.org/10.1016/j.chom.2014.02.005.
7. Dinakaran V, Mandape SN, Shuba K, Pratap S, Sakhare SS, Tabatabai MA, Smoot DT, Farmer-Dixon CM, Kesavalu LN, Adunyah SE, Southerland JH, Gangula PR. 2018. Identification of specific oral and gut pathogens in full thickness colon of colitis patients: implications for colon motility. Front Microbiol 9:3220. https://doi.org/10.3389/fmicb.2018.03220.
8. Xun Z, Zhang Q, Xu T, Chen N, Chen F. 2018. Dysbiosis and ecotypes of the salivary microbiome associated with inflammatory bowel diseases and the assistance in diagnosis of diseases using oral bacterial profiles. Front Microbiol 9:1136. https://doi.org/10.3389/fmicb.2018.01136.
9. Schirmer M, Denson L, Vlamakis H, Franzosa EA, Thomas S, Gotman NM, Rufo P, Baker SS, Sauer C, Markowitz J, Pfefferkorn M, Oliva-Hemker M, Rosh J, Otley A, Boyle B, Mack D, Baldassano R, Keljo D, LeLeiko N, Heyman M, Griffiths A, Patel AS, Noe J, Kugathasan S, Walters T, Huttenhower C, Hyams J, Xavier RJ. 2018. Compositional and temporal changes in the gut microbiome of pediatric ulcerative colitis patients are linked to disease course. Cell Host Microbe 24:600–610.e4. https://doi.org/10.1016/j.chom.2018.09.009.
10. Ohkusa T, Okayasu I, Ogihara T, Morita K, Ogawa M, Sato N. 2003. Induction of experimental ulcerative colitis by *Fusobacterium varium* isolated from colonic mucosa of patients with ulcerative colitis. Gut 52:79–83. https://doi.org/10.1136/gut.52.1.79.
11. Strauss J, Kaplan GG, Beck PL, Rioux K, Panaccione R, Devinney R, Lynch T, Allen-Vercoe E. 2011. Invasive potential of gut mucosa-derived *Fusobacterium nucleatum* positively correlates with IBD status of the host. Inflamm Bowel Dis 17:1971–1978. https://doi.org/10.1002/ibd.21606.
12. Strauss J, White A, Ambrose C, McDonald J, Allen-Vercoe E. 2008. Phenotypic and genotypic analyses of clinical *Fusobacterium nucleatum* and *Fusobacterium periodonticum* isolates from the human gut. Anaerobe 14:301–309. https://doi.org/10.1016/j.anaerobe.2008.12.003.
13. Tahara T, Shibata T, Kawamura T, Okubo M, Ichikawa Y, Sumi K, Miyata M, Ishizuka T, Nakamura M, Nagasaka M, Nakagawa Y, Ohmiya N, Arisawa T, Hirata I. 2015. *Fusobacterium* detected in colonic biopsy and clinicopathological features of ulcerative colitis in Japan. Dig Dis Sci 60:205–210. https://doi.org/10.1007/s10620-014-3316-y.
14. Lee Y, Eun CS, Lee AR, Park CH, Han DS. 2016. *Fusobacterium* isolates recovered from colonic biopsies of inflammatory bowel disease patients in Korea. Ann Lab Med 36:387–389. https://doi.org/10.3343/alm.2016.36.4.387.

15. Yao P, Cui M, Wang H, Gao H, Wang L, Yang T, Cheng Y. 2016. Quantitative analysis of intestinal flora of Uygur and Han ethnic Chinese patients with ulcerative colitis. Gastroenterol Res Pract 2016:9186232. https://doi.org/10.1155/2016/9186232.

16. Ohkusa T, Yoshida T, Sato N, Watanabe S, Tajiri H, Okayasu I. 2009. Commensal bacteria can enter colonic epithelial cells and induce proinflammatory cytokine secretion: a possible pathogenic mechanism of ulcerative colitis. J Med Microbiol 58:535–545. https://doi.org/10.1099/jmm.0.005801-0.

17. Shaw KA, Bertha M, Hofmekler T, Chopra P, Vatanen T, Srivatsa A, Prince J, Kumar A, Sauer C, Zwick ME, Satten GA, Kostic AD, Mulle JG, Xavier RJ, Kugathasan S. 2016. Dysbiosis, inflammation, and response to treatment: a longitudinal study of pediatric subjects with newly diagnosed inflammatory bowel disease. Genome Med 8:75. https://doi.org/10.1186/s13073-016-0331-y.

18. Kelsen J, Bittinger K, Pauly-Hubbard H, Posivak L, Grunberg S, Baldassano R, Lewis JD, Wu GD, Bushman FD. 2015. Alterations of the subgingival microbiota in pediatric Crohn's disease studied longitudinally in discovery and validation cohorts. Inflamm Bowel Dis 21:2797–2805. https://doi.org/10.1097/MIB.0000000000000557.

19. Pascal V, Pozuelo M, Borruel N, Casellas F, Campos D, Santiago A, Martinez X, Varela E, Sarrabayrouse G, Machiels K, Vermeire S, Sokol H, Guarner F, Manichanh C. 2017. A microbial signature for Crohn's disease. Gut 66:813–822. https://doi.org/10.1136/gutjnl-2016-313235.

20. Metwaly A, Dunkel A, Waldschmitt N, Raj ACD, Lagkouvardos I, Corraliza AM, Mayorgas A, Martinez-Medina M, Reiter S, Schloter M, Hofmann T, Allez M, Panes J, Salas A, Haller D. 2020. Integrated microbiota and metabolite profiles link Crohn's disease to sulfur metabolism. Nat Commun 11:4322. https://doi.org/10.1038/s41467-020-17956-1.

21. de Meij TGJ, de Groot EFJ, Peeters CFW, de Boer NKH, Kneepkens CMF, Eck A, Benninga MA, Savelkoul PHM, van Bodegraven AA, Budding AE. 2018. Variability of core microbiota in newly diagnosed treatment-naive paediatric inflammatory bowel disease patients. PLoS One 13:e0197649. https://doi.org/10.1371/journal.pone.0197649.

22. Hagelskjaer Kristensen L, Prag J. 2008. Lemierre's syndrome and other disseminated *Fusobacterium necrophorum* infections in Denmark: a prospective epidemiological and clinical survey. Eur J Clin Microbiol Infect Dis 27:779–789. https://doi.org/10.1007/s10096-008-0496-4.

23. Nohrstrom E, Mattila T, Pettila V, Kuusela P, Carlson P, Kentala E, Mattila PS. 2011. Clinical spectrum of bacteraemic *Fusobacterium* infections: from septic shock to nosocomial bacteraemia. Scand J Infect Dis 43:463–470. https://doi.org/10.3109/00365548.2011.565071.

24. Bolstad AI, Jensen HB, Bakken V. 1996. Taxonomy, biology, and periodontal aspects of *Fusobacterium nucleatum*. Clin Microbiol Rev 9:55–71. https://doi.org/10.1128/CMR.9.1.55-71.1996.

25. Han YW, Shen T, Chung P, Buhimschi IA, Buhimschi CS. 2009. Uncultivated bacteria as etiologic agents of intra-amniotic inflammation leading to preterm birth. J Clin Microbiol 47:38–47. https://doi.org/10.1128/JCM.01206-08.

26. Afra K, Laupland K, Leal J, Lloyd T, Gregson D. 2013. Incidence, risk factors, and outcomes of *Fusobacterium* species bacteremia. BMC Infect Dis 13:264. https://doi.org/10.1186/1471-2334-13-264.

27. Swidsinski A, Dorffel Y, Loening-Baucke V, Tertychnyy A, Biche-Ool S, Stonogin S, Guo Y, Sun ND. 2012. Mucosal invasion by fusobacteria is a common feature of acute appendicitis in Germany, Russia, and China. Saudi J Gastroenterol 18:55–58. https://doi.org/10.4103/1319-3767.91734.

28. Swidsinski A, Dorffel Y, Loening-Baucke V, Theissig F, Ruckert JC, Ismail M, Rau WA, Gaschler D, Weizenegger M, Kuhn S, Schilling J, Dorffel WV. 2011. Acute appendicitis is characterised by local invasion with *Fusobacterium nucleatum*/necrophorum. Gut 60:34–40. https://doi.org/10.1136/gut.2009.191320.

29. Kostic AD, Chun E, Robertson L, Glickman JN, Gallini CA, Michaud M, Clancy TE, Chung DC, Lochhead P, Hold GL, El-Omar EM, Brenner D, Fuchs CS, Meyerson M, Garrett WS. 2013. *Fusobacterium nucleatum* potentiates intestinal tumorigenesis and modulates the tumor-immune microenvironment. Cell Host Microbe 14:207–215. https://doi.org/10.1016/j.chom.2013.07.007.

30. McCoy AN, Araujo-Perez F, Azcarate-Peril A, Yeh JJ, Sandler RS, Keku TO. 2013. *Fusobacterium* is associated with colorectal adenomas. PLoS One 8:e53653. https://doi.org/10.1371/journal.pone.0053653.

31. Liu J, Hsieh CL, Gelincik O, Devolder B, Sei S, Zhang S, Lipkin SM, Chang YF. 2019. Proteomic characterization of outer membrane vesicles from gut mucosa-derived *Fusobacterium nucleatum*. J Proteomics 195:125–137. https://doi.org/10.1016/j.jprot.2018.12.029.

32. Wu Y, Wu J, Chen T, Li Q, Peng W, Li H, Tang X, Fu X. 2018. *Fusobacterium nucleatum* potentiates intestinal tumorigenesis in mice via a Toll-like receptor 4/p21-activated kinase 1 cascade. Dig Dis Sci 63:1210–1218. https://doi.org/10.1007/s10620-018-4999-2.

33. Zhou Z, Chen J, Yao H, Hu H. 2018. *Fusobacterium* and colorectal cancer. Front Oncol 8:371. https://doi.org/10.3389/fonc.2018.00371.

34. Peng BJ, Cao CY, Li W, Zhou YJ, Zhang Y, Nie YQ, Cao YW, Li YY. 2018. Diagnostic performance of intestinal *Fusobacterium nucleatum* in colorectal cancer: a meta-analysis. Chin Med J (Engl) 131:1349–1356. https://doi.org/10.4103/0366-6999.232814.

35. Kostic AD, Gevers D, Pedamallu CS, Michaud M, Duke F, Earl AM, Ojesina AI, Jung J, Bass AJ, Tabernero J, Baselga J, Liu C, Shivdasani RA, Ogino S, Birren BW, Huttenhower C, Garrett WS, Meyerson M. 2012. Genomic analysis identifies association of Fusobacterium with colorectal carcinoma. Genome Res 22:292–298. https://doi.org/10.1101/gr.126573.111.

36. Jayasimhan D, Wu L, Huggan P. 2017. Fusobacterial liver abscess: a case report and review of the literature. BMC Infect Dis 17:440. https://doi.org/10.1186/s12879-017-2548-9.

37. Hannoodi F, Sabbagh H, Kulairi Z, Kumar S. 2017. A rare case of *Fusobacterium necrophorum* liver abscesses. Clin Pract 7:928. https://doi.org/10.4081/cp.2017.928.

38. Garcia-Carretero R. 2019. Bacteraemia and multiple liver abscesses due to *Fusobacterium nucleatum* in a patient with oropharyngeal malignancy. BMJ Case Rep 12:e228237. https://doi.org/10.1136/bcr-2018-228237.

39. Pereira P, Aho V, Arola J, Boyd S, Jokelainen K, Paulin L, Auvinen P, Farkkila M. 2017. Bile microbiota in primary sclerosing cholangitis: impact on disease progression and development of biliary dysplasia. PLoS One 12:e0182924. https://doi.org/10.1371/journal.pone.0182924.

40. Sabino J, Vieira-Silva S, Machiels K, Joossens M, Falony G, Ballet V, Ferrante M, Van Assche G, Van der Merwe S, Vermeire S, Raes J. 2016. Primary sclerosing cholangitis is characterised by intestinal dysbiosis independent from IBD. Gut 65:1681–1689. https://doi.org/10.1136/gutjnl-2015-311004.

41. Torres J, Palmela C, Brito H, Bao X, Ruiqi H, Moura-Santos P, Pereira da Silva J, Oliveira A, Vieira C, Perez K, Itzkowitz SH, Colombel JF, Humbert L, Rainteau D, Cravo M, Rodrigues CM, Hu J. 2018. The gut microbiota, bile acids and their correlation in primary sclerosing cholangitis associated with inflammatory bowel disease. United Eur Gastroenterol J 6:112–122. https://doi.org/10.1177/2050640617708953.

42. Macfarlane S, Furrie E, Macfarlane GT, Dillon JF. 2007. Microbial colonization of the upper gastrointestinal tract in patients with Barrett's esophagus. Clin Infect Dis 45:29–38. https://doi.org/10.1086/518578.

43. Yang L, Lu X, Nossa CW, Francois F, Peek RM, Pei Z. 2009. Inflammation and intestinal metaplasia of the distal esophagus are associated with alterations in the microbiome. Gastroenterology 137:588–597. https://doi.org/10.1053/j.gastro.2009.04.046.

44. Liu N, Ando T, Ishiguro K, Maeda O, Watanabe O, Funasaka K, Nakamura M, Miyahara R, Ohmiya N, Goto H. 2013. Characterization of bacterial biota in the distal esophagus of Japanese patients with reflux esophagitis and Barrett's esophagus. BMC Infect Dis 13:130. https://doi.org/10.1186/1471-2334-13-130.

45. Gall A, Fero J, McCoy C, Claywell BC, Sanchez CA, Blount PL, Li X, Vaughan TL, Matsen FA, Reid BJ, Salama NR. 2015. Bacterial composition of the human upper gastrointestinal tract microbiome is dynamic and associated with genomic instability in a Barrett's esophagus cohort. PLoS One 10:e0129055. https://doi.org/10.1371/journal.pone.0129055.

46. Ziganshina EE, Sagitov II, Akhmetova RF, Saleeva GT, Kiassov AP, Gogoleva NE, Shagimardanova EI, Ziganshin AM. 2020. Comparison of the microbiota and inorganic anion content in the saliva of patients with gastroesophageal reflux disease and gastroesophageal reflux disease-free individuals. Biomed Res Int 2020:2681791. https://doi.org/10.1155/2020/2681791.

47. Gonzalez OA, Li M, Ebersole JL, Huang CB. 2010. HIV-1 reactivation induced by the periodontal pathogens *Fusobacterium nucleatum* and *Porphyromonas gingivalis* involves Toll-like receptor 2 [corrected] and 9 activation in monocytes/macrophages. Clin Vaccine Immunol 17:1417–1427. https://doi.org/10.1128/CVI.00009-10.

48. Lee SC, Chua LL, Yap SH, Khang TF, Leng CY, Raja Azwa RI, Lewin SR, Kamarulzaman A, Woo YL, Lim YAL, Loke P, Rajasuriar R. 2018. Enrichment of gut-derived *Fusobacterium* is associated with suboptimal immune recovery in HIV-infected individuals. Sci Rep 8:14277. https://doi.org/10.1038/s41598-018-32585-x.

49. McHardy IH, Li X, Tong M, Ruegger P, Jacobs J, Borneman J, Anton P, Braun J. 2013. HIV Infection is associated with compositional and

functional shifts in the rectal mucosal microbiota. Microbiome 1:26. https://doi.org/10.1186/2049-2618-1-26.

50. Lages EJ, Costa FO, Cortelli SC, Cortelli JR, Cota LO, Cyrino RM, Lages EM, Nobre-Franco GC, Brito JA, Gomez RS. 2015. Alcohol consumption and periodontitis: quantification of periodontal pathogens and cytokines. J Periodontol 86:1058–1068. https://doi.org/10.1902/jop.2015.150087.

51. Musrati AA, Fteita D, Paranko J, Kononen E, Gursoy UK. 2016. Morphological and functional adaptations of *Fusobacterium nucleatum* exposed to human neutrophil Peptide-1. Anaerobe 39:31–38. https://doi.org/10.1016/j.anaerobe.2016.02.008.

52. Elliott CL, Allport VC, Loudon JA, Wu GD, Bennett PR. 2001. Nuclear factor-κB is essential for up-regulation of interleukin-8 expression in human amnion and cervical epithelial cells. Mol Hum Reprod 7:787–790. https://doi.org/10.1093/molehr/7.8.787.

53. Drummond CG, Bolock AM, Ma C, Luke CJ, Good M, Coyne CB. 2017. Enteroviruses infect human enteroids and induce antiviral signaling in a cell lineage-specific manner. Proc Natl Acad Sci U S A 114:1672–1677. https://doi.org/10.1073/pnas.1617363114.

54. Ruan W, Engevik MA, Chang-Graham AL, Danhof HA, Goodwin A, Engevik KA, Shi Z, Hall A, Rienzi SCD, Venable S, Britton RA, Hyser J, Versalovic J. 2020. Enhancing responsiveness of human jejunal enteroids to host and microbial stimuli. J Physiol 598:3085–3105. https://doi.org/10.1113/JP279423.

55. Chang-Graham AL, Danhof HA, Engevik MA, Tomaro-Duchesneau C, Karandikar UC, Estes MK, Versalovic J, Britton RA, Hyser JM. 2019. Human intestinal enteroids with inducible neurogenin-3 expression as a novel model of gut hormone secretion. Cell Mol Gastroenterol Hepatol 8:209–229. https://doi.org/10.1016/j.jcmgh.2019.04.010.

56. Engevik AC, Engevik MA. 2021. Exploring the impact of intestinal ion transport on the gut microbiota. Comput Struct Biotechnol J 19:134–144. https://doi.org/10.1016/j.csbj.2020.12.008.

57. Engevik M, Danhof HA, Auchtung J, Endres BT, Ruan W, Basseres E, Engevik AC, Wu Q, Nicholson M, Luna RA, Garey KW, Crawford SE, Estes MK, Lux R, Yacyshyn MB, Yacyshyn B, Savidge T, Britton RA, Versalovic J. 2020. *Fusobacterium nucleatum* adheres to Clostridioides difficile via the RadD adhesin to enhance biofilm formation in intestinal mucus. Gastroenterology https://doi.org/10.1053/j.gastro.2020.11.034.

58. Collins J, Auchtung JM, Schaefer L, Eaton KA, Britton RA. 2015. Humanized microbiota mice as a model of recurrent *Clostridium difficile* disease. Microbiome 3:35. https://doi.org/10.1186/s40168-015-0097-2.

59. Bullman S, Pedamallu CS, Sicinska E, Clancy TE, Zhang X, Cai D, Neuberg D, Huang K, Guevara F, Nelson T, Chipashvili O, Hagan T, Walker M, Ramachandran A, Diosdado B, Serna G, Mulet N, Landolfi S, Ramon YCS, Fasani R, Aguirre AJ, Ng K, Elez E, Ogino S, Tabernero J, Fuchs CS, Hahn WC, Nuciforo P, Meyerson M. 2017. Analysis of *Fusobacterium* persistence and antibiotic response in colorectal cancer. Science 358:1443–1448. https://doi.org/10.1126/science.aal5240.

60. Li YY, Ge QX, Cao J, Zhou YJ, Du YL, Shen B, Wan YJ, Nie YQ. 2016. Association of *Fusobacterium nucleatum* infection with colorectal cancer in Chinese patients. WJG 22:3227–3233. https://doi.org/10.3748/wjg.v22.i11.3227.

61. Ito M, Kanno S, Nosho K, Sukawa Y, Mitsuhashi K, Kurihara H, Igarashi H, Takahashi T, Tachibana M, Takahashi H, Yoshii S, Takenouchi T, Hasegawa T, Okita K, Hirata K, Maruyama R, Suzuki H, Imai K, Yamamoto H, Shinomura Y. 2015. Association of *Fusobacterium nucleatum* with clinical and molecular features in colorectal serrated pathway. Int J Cancer 137:1258–1268. https://doi.org/10.1002/ijc.29488.

62. Shang FM, Liu HL. 2018. *Fusobacterium nucleatum* and colorectal cancer: a review. World J Gastrointest Oncol 10:71–81. https://doi.org/10.4251/wjgo.v10.i3.71.

63. Flanagan L, Schmid J, Ebert M, Soucek P, Kunicka T, Liska V, Bruha J, Neary P, Dezeeuw N, Tommasino M, Jenab M, Prehn JH, Hughes DJ. 2014. *Fusobacterium nucleatum* associates with stages of colorectal neoplasia development, colorectal cancer and disease outcome. Eur J Clin Microbiol Infect Dis 33:1381–1390. https://doi.org/10.1007/s10096-014-2081-3.

64. Castellarin M, Warren RL, Freeman JD, Dreolini L, Krzywinski M, Strauss J, Barnes R, Watson P, Allen-Vercoe E, Moore RA, Holt RA. 2012. *Fusobacterium nucleatum* infection is prevalent in human colorectal carcinoma. Genome Res 22:299–306. https://doi.org/10.1101/gr.126516.111.

65. Ahn J, Sinha R, Pei Z, Dominianni C, Wu J, Shi J, Goedert JJ, Hayes RB, Yang L. 2013. Human gut microbiome and risk for colorectal cancer. J Natl Cancer Inst 105:1907–1911. https://doi.org/10.1093/jnci/djt300.

66. Koido S, Ohkusa T, Kajiura T, Shinozaki J, Suzuki M, Saito K, Takakura K, Tsukinaga S, Odahara S, Yukawa T, Mitobe J, Kajihara M, Uchiyama K, Arakawa H, Tajiri H. 2014. Long-term alteration of intestinal microbiota in patients with ulcerative colitis by antibiotic combination therapy. PLoS One 9:e86702. https://doi.org/10.1371/journal.pone.0086702.

67. Lee EY, Choi DS, Kim KP, Gho YS. 2008. Proteomics in gram-negative bacterial outer membrane vesicles. Mass Spectrom Rev 27:535–555. https://doi.org/10.1002/mas.20175.

68. Unal CM, Schaar V, Riesbeck K. 2011. Bacterial outer membrane vesicles in disease and preventive medicine. Semin Immunopathol 33:395–408. https://doi.org/10.1007/s00281-010-0231-y.

69. Jan AT. 2017. Outer membrane vesicles (OMVs) of Gram-negative bacteria: a perspective update. Front Microbiol 8:1053. https://doi.org/10.3389/fmicb.2017.01053.

70. Ellis TN, Kuehn MJ. 2010. Virulence and immunomodulatory roles of bacterial outer membrane vesicles. Microbiol Mol Biol Rev 74:81–94. https://doi.org/10.1128/MMBR.00031-09.

71. Liu H, Redline RW, Han YW. 2007. *Fusobacterium nucleatum* induces fetal death in mice via stimulation of TLR4-mediated placental inflammatory response. J Immunol 179:2501–2508. https://doi.org/10.4049/jimmunol.179.4.2501.

72. Park SR, Kim DJ, Han SH, Kang MJ, Lee JY, Jeong YJ, Lee SJ, Kim TH, Ahn SG, Yoon JH, Park JH. 2014. Diverse Toll-like receptors mediate cytokine production by *Fusobacterium nucleatum* and *Aggregatibacter actinomycetemcomitans* in macrophages. Infect Immun 82:1914–1920. https://doi.org/10.1128/IAI.01226-13.

73. Bui FQ, Johnson L, Roberts J, Hung SC, Lee J, Atanasova KR, Huang PR, Yilmaz O, Ojcius DM. 2016. *Fusobacterium nucleatum* infection of gingival epithelial cells leads to NLRP3 inflammasome-dependent secretion of IL-1β and the danger signals ASC and HMGB1. Cell Microbiol 18:970–981. https://doi.org/10.1111/cmi.12560.

74. Han YW, Shi W, Huang GT, Kinder Haake S, Park NH, Kuramitsu H, Genco RJ. 2000. Interactions between periodontal bacteria and human oral epithelial cells: *Fusobacterium nucleatum* adheres to and invades epithelial cells. Infect Immun 68:3140–3146. https://doi.org/10.1128/iai.68.6.3140-3146.2000.

75. Signat B, Roques C, Poulet P, Duffaut D. 2011. *Fusobacterium nucleatum* in periodontal health and disease. Curr Issues Mol Biol 13:25–36.

76. Dharmani P, Strauss J, Ambrose C, Allen-Vercoe E, Chadee K. 2011. *Fusobacterium nucleatum* infection of colonic cells stimulates MUC2 mucin and tumor necrosis factor alpha. Infect Immun 79:2597–2607. https://doi.org/10.1128/IAI.05118-11.

77. Frank DN, St Amand AL, Feldman RA, Boedeker EC, Harpaz N, Pace NR. 2007. Molecular-phylogenetic characterization of microbial community imbalances in human inflammatory bowel diseases. Proc Natl Acad Sci U S A 104:13780–13785. https://doi.org/10.1073/pnas.0706625104.

78. Kostic AD, Xavier RJ, Gevers D. 2014. The microbiome in inflammatory bowel disease: current status and the future ahead. Gastroenterology 146:1489–1499. https://doi.org/10.1053/j.gastro.2014.02.009.

79. Shen ZH, Zhu CX, Quan YS, Yang ZY, Wu S, Luo WW, Tan B, Wang XY. 2018. Relationship between intestinal microbiota and ulcerative colitis: mechanisms and clinical application of probiotics and fecal microbiota transplantation. World J Gastroenterol 24:5–14. https://doi.org/10.3748/wjg.v24.i1.5.

80. Loh G, Blaut M. 2012. Role of commensal gut bacteria in inflammatory bowel diseases. Gut Microbes 3:544–555. https://doi.org/10.4161/gmic.22156.

81. Wang T, Cai G, Qiu Y, Fei N, Zhang M, Pang X, Jia W, Cai S, Zhao L. 2012. Structural segregation of gut microbiota between colorectal cancer patients and healthy volunteers. ISME J 6:320–329. https://doi.org/10.1038/ismej.2011.109.

82. Shen XJ, Rawls JF, Randall T, Burcal L, Mpande CN, Jenkins N, Jovov B, Abdo Z, Sandler RS, Keku TO. 2010. Molecular characterization of mucosal adherent bacteria and associations with colorectal adenomas. Gut Microbes 1:138–147. https://doi.org/10.4161/gmic.1.3.12360.

83. Rinninella E, Raoul P, Cintoni M, Franceschi F, Miggiano GAD, Gasbarrini A, Mele MC. 2019. What is the healthy gut microbiota composition? A changing ecosystem across age, environment, diet, and diseases. Microorganisms 7:14. https://doi.org/10.3390/microorganisms7010014.

84. Drewes JL, White JR, Dejea CM, Fathi P, Iyadorai T, Vadivelu J, Roslani AC, Wick EC, Mongodin EF, Loke MF, Thulasi K, Gan HM, Goh KL, Chong HY, Kumar S, Wanyiri JW, Sears CL. 2017. High-resolution bacterial 16S rRNA gene profile meta-analysis and biofilm status reveal common colorectal

cancer consortia. NPJ Biofilms Microbiomes 3:34. https://doi.org/10.1038/s41522-017-0040-3.

85. Yang Y, Misra BB, Liang L, Bi D, Weng W, Wu W, Cai S, Qin H, Goel A, Li X, Ma Y. 2019. Integrated microbiome and metabolome analysis reveals a novel interplay between commensal bacteria and metabolites in colorectal cancer. Theranostics 9:4101–4114. https://doi.org/10.7150/thno.35186.

86. Bennett KW, Eley A. 1993. Fusobacteria: new taxonomy and related diseases. J Med Microbiol 39:246–254. https://doi.org/10.1099/00222615-39-4-246.

87. Kolenbrander PE, Andersen RN, Moore LV. 1989. Coaggregation of *Fusobacterium nucleatum*, *Selenomonas flueggei*, *Selenomonas infelix*, *Selenomonas noxia*, and *Selenomonas sputigena* with strains from 11 genera of oral bacteria. Infect Immun 57:3194–3203. https://doi.org/10.1128/IAI.57.10.3194-3203.1989.

88. Karched M, Bhardwaj RG, Asikainen SE. 2015. Coaggregation and biofilm growth of *Granulicatella* spp. with *Fusobacterium nucleatum* and *Aggregatibacter actinomycetemcomitans*. BMC Microbiol 15:114. https://doi.org/10.1186/s12866-015-0439-z.

89. Nagayama M, Sato M, Yamaguchi R, Tokuda C, Takeuchi H. 2001. Evaluation of co-aggregation among *Streptococcus mitis*, *Fusobacterium nucleatum*, and *Porphyromonas gingivalis*. Lett Appl Microbiol 33:122–125. https://doi.org/10.1046/j.1472-765x.2001.00964.x.

90. Grimaudo NJ, Nesbitt WE. 1997. Coaggregation of *Candida albicans* with oral *Fusobacterium* species. Oral Microbiol Immunol 12:168–173. https://doi.org/10.1111/j.1399-302x.1997.tb00374.x.

91. Ledder RG, Timperley AS, Friswell MK, Macfarlane S, McBain AJ. 2008. Coaggregation between and among human intestinal and oral bacteria. FEMS Microbiol Ecol 66:630–636. https://doi.org/10.1111/j.1574-6941.2008.00525.x.

92. Thurnheer T, Karygianni L, Flury M, Belibasakis GN. 2019. *Fusobacterium* species and subspecies differentially affect the composition and architecture of supra- and subgingival biofilms models. Front Microbiol 10:1716. https://doi.org/10.3389/fmicb.2019.01716.

93. He X, Hu W, Kaplan CW, Guo L, Shi W, Lux R. 2012. Adherence to streptococci facilitates *Fusobacterium nucleatum* integration into an oral microbial community. Microb Ecol 63:532–542. https://doi.org/10.1007/s00248-011-9989-2.

94. Khemaleelakul S, Baumgartner JC, Pruksakorn S. 2006. Autoaggregation and coaggregation of bacteria associated with acute endodontic infections. J Endod 32:312–318. https://doi.org/10.1016/j.joen.2005.10.003.

95. Merritt J, Niu G, Okinaga T, Qi F. 2009. Autoaggregation response of *Fusobacterium nucleatum*. Appl Environ Microbiol 75:7725–7733. https://doi.org/10.1128/AEM.00916-09.

96. Park J, Shokeen B, Haake SK, Lux R. 2016. Characterization of *Fusobacterium nucleatum* ATCC 23726 adhesins involved in strain-specific attachment to *Porphyromonas gingivalis*. Int J Oral Sci 8:138–144. https://doi.org/10.1038/ijos.2016.27.

97. Zilm PS, Rogers AH. 2007. Co-adhesion and biofilm formation by *Fusobacterium nucleatum* in response to growth pH. Anaerobe 13:146–152. https://doi.org/10.1016/j.anaerobe.2007.04.005.

98. Engevik MA, Luk B, Chang-Graham AL, Hall A, Herrmann B, Ruan W, Endres BT, Shi Z, Garey KW, Hyser JM, Versalovic J. 2019. *Bifidobacterium dentium* fortifies the intestinal mucus layer via autophagy and calcium signaling pathways. mBio 10:e01087-19. https://doi.org/10.1128/mBio.01087-19.

99. Engevik MA, Banks LD, Engevik KA, Chang-Graham AL, Perry JL, Hutchinson DS, Ajami NJ, Petrosino JF, Hyser JM. 2020. Rotavirus infection induces glycan availability to promote ileum-specific changes in the microbiome aiding rotavirus virulence. Gut Microbes 11:1324–1347. https://doi.org/10.1080/19490976.2020.1754714.

100. Bradford MM. 1976. A rapid and sensitive method for the quantitation of microgram quantities of protein utilizing the principle of protein-dye binding. Anal Biochem 72:248–254. https://doi.org/10.1006/abio.1976.9999.

101. Yu Y, Ge N, Xie M, Sun W, Burlingame S, Pass AK, Nuchtern JG, Zhang D, Fu S, Schneider MD, Fan J, Yang J. 2008. Phosphorylation of Thr-178 and Thr-184 in the TAK1 T-loop is required for interleukin (IL)-1-mediated optimal NF-κB and AP-1 activation as well as IL-6 gene expression. J Biol Chem 283:24497–24505. https://doi.org/10.1074/jbc.M802825200.

102. Sato T, Stange DE, Ferrante M, Vries RG, Van Es JH, Van den Brink S, Van Houdt WJ, Pronk A, Van Gorp J, Siersema PD, Clevers H. 2011. Long-term expansion of epithelial organoids from human colon, adenoma, adenocarcinoma, and Barrett's epithelium. Gastroenterology 141:1762–1772. https://doi.org/10.1053/j.gastro.2011.07.050.

103. Saxena K, Blutt SE, Ettayebi K, Zeng XL, Broughman JR, Crawford SE, Karandikar UC, Sastri NP, Conner ME, Opekun AR, Graham DY, Qureshi W, Sherman V, Foulke-Abel J, In J, Kovbasnjuk O, Zachos NC, Donowitz M, Estes MK. 2016. Human intestinal enteroids: a new model to study human rotavirus infection, host restriction, and pathophysiology. J Virol 90:43–56. https://doi.org/10.1128/JVI.01930-15.

104. Engevik MA, Morra CN, Roth D, Engevik K, Spinler JK, Devaraj S, Crawford SE, Estes MK, Kalkum M, Versalovic J. 2019. Microbial metabolic capacity for intestinal folate production and modulation of host folate receptors. Front Microbiol 10:2305. https://doi.org/10.3389/fmicb.2019.02305.

105. VanDussen KL, Marinshaw JM, Shaikh N, Miyoshi H, Moon C, Tarr PI, Ciorba MA, Stappenbeck TS. 2015. Development of an enhanced human gastrointestinal epithelial culture system to facilitate patient-based assays. Gut 64:911–920. https://doi.org/10.1136/gutjnl-2013-306651.

106. Ettayebi K, Crawford SE, Murakami K, Broughman JR, Karandikar U, Tenge VR, Neill FH, Blutt SE, Zeng XL, Qu L, Kou B, Opekun AR, Burrin D, Graham DY, Ramani S, Atmar RL, Estes MK. 2016. Replication of human noroviruses in stem cell-derived human enteroids. Science 353:1387–1393. https://doi.org/10.1126/science.aaf5211.

107. Chang-Graham AL, Danhof HA, Engevik MA, Tomaro-Duchesneau C, Karandikar UC, Estes MK, Versalovic J, Britton RA, Hyser JM. 2019. Human intestinal enteroids with inducible neurogenin-3 expression as a novel model of gut hormone secretion. Cell Mol Gastroenterol Hepatol 8:209–229. https://doi.org/10.1016/j.jcmgh.2019.04.010.

108. Zou WY, Blutt SE, Crawford SE, Ettayebi K, Zeng XL, Saxena K, Ramani S, Karandikar UC, Zachos NC, Estes MK. 2017. Human intestinal enteroids: new models to study gastrointestinal virus infections. Methods Mol Biol 1576:229–247. https://doi.org/10.1007/7651_2017_1.

109. Rajan A, Vela L, Zeng XL, Yu X, Shroyer N, Blutt SE, Poole NM, Carlin LG, Nataro JP, Estes MK, Okhuysen PC, Maresso AW. 2018. Novel segment- and host-specific patterns of enteroaggregative *Escherichia coli* adherence to human intestinal enteroids. mBio 9:e02419-17. https://doi.org/10.1128/mBio.02419-17.

110. Sigge A, Essig A, Wirths B, Fickweiler K, Kaestner N, Wellinghausen N, Poppert S. 2007. Rapid identification of *Fusobacterium nucleatum* and *Fusobacterium necrophorum* by fluorescence *in situ* hybridization. Diagn Microbiol Infect Dis 58:255–259. https://doi.org/10.1016/j.diagmicrobio.2007.01.001.

111. Meenderink LM, Gaeta IM, Postema MM, Cencer CS, Chinowsky CR, Krystofiak ES, Millis BA, Tyska MJ. 2019. Actin dynamics drive microvillar motility and clustering during brush border assembly. Dev Cell 50:545–556.e4. https://doi.org/10.1016/j.devcel.2019.07.008.

112. Engevik MA, Aihara E, Montrose MH, Shull GE, Hassett DJ, Worrell RT. 2013. Loss of NHE3 alters gut microbiota composition and influences *Bacteroides thetaiotaomicron* growth. Am J Physiol Gastrointest Liver Physiol 305:G697–G711. https://doi.org/10.1152/ajpgi.00184.2013.